Bioactive Materials 13 (2022) 161–178

Contents lists available at ScienceDirect

Bioactive Materials

journal homepage: www.keaipublishing.com/en/journals/bioactive-materials

# Advancing dental implants: Bioactive and therapeutic modifications of zirconia

Divya Chopra, Anjana Jayasree [1], Tianqi Guo [1], Karan Gulati [*], Sašo Ivanovski [*]

*The University of Queensland, School of Dentistry, Herston QLD, 4006, Australia*

ARTICLE INFO

*Keywords:*
Zirconium
Zirconia
Implants
Surface modification
Osseointegration
Bioactivity
Local therapy

ABSTRACT

Zirconium-based implants have gained popularity in the dental implant field owing to their corrosion resistance and biocompatibility, attributed to the formation of a native zirconia ($ZrO_2$) film. However, enhanced bioactivity and local therapy from such implants are desirable to enable the earlier establishment and improved long-term maintenance of implant integration, especially in compromised patient conditions. As a result, surface modification of zirconium-based implants have been performed using various physical, chemical and biological techniques at the macro-, micro-, and nano-scales. In this extensive review, we discuss and detail the development of Zr implants covering the spectrum from past and present advancements to future perspectives, arriving at the next generation of highly bioactive and therapeutic nano-engineered Zr-based implants. The review provides in-depth knowledge of the bioactive/therapeutic value of surface modification of Zr implants in dental implant applications focusing on clinical translation.

## 1. Introduction

Biocompatible and corrosion-resistant zirconium (Zr) has gained popularity as a materialchoice for orthopaedic and dental implants [2,3]. In just two decades since $ZrO_2$ (Zirconia) was introduced as a biomedical grade metal, around 600,000 femoral heads have been implanted worldwide, and the market for dental implants has increased by more than 12% per year [6]. While titanium (Ti) dental implants demonstrate excellent biocompatibility and have been the popular choice clinically, the following limitations associated with Ti have led to a search for an alternative material choice [7]:

- Grey colour (reduced aesthetic outcomes) [8].
- Development of hypersensitivity to Ti [9].
- Accumulation of Ti particles in lymph nodes and organs [10].
- Corrosion in the presence of fluoride or metal alloys in saliva [11].
- Oxidation induced by bacterial biofilms in acidic conditions [12].

Initially used for fabricating crowns and abutments, Zirconia ceramics (superior biomechanical characteristics as compared to other ceramics like alumina) have become a popular choice for dental implants [13]. It has been established that micro-rough $ZrO_2$ implants are equivalent to the 'gold standard' Ti micro-rough implants in terms of osseointegration capacity [14].

The following attributes are the key reasons for preferring $ZrO_2$ over Ti as a dental implant material choice:

- White, opaque colour
- Reduced affinity to bacterial plaque, reduced inflammatory infiltrate and favourable soft-tissue integration [15], translating into reduced risk for peri-implant diseases
- Reduced thermal conductivity, high flexural strength and high fracture toughness
- In comparison to other metals, like stainless steel, CoCr alloys and Ti alloys, $ZrO_2$ is non-magnetic [16], which means it does not interfere with standard diagnostic techniques, such as magnetic resonance imaging (MRI) [17].

Clinically, Zr-based implants have shown promising outcomes with low ion release, lower cytotoxicity, favourable biocompatibility, and good osseointegration capability compared to Ti [18].

Zr readily forms biocompatible $ZrO_2$ upon exposure to oxygen and

Peer review under responsibility of KeAi Communications Co., Ltd.
* Corresponding authors. School of Dentistry, University of Queensland, 288 Herston Road, Herston QLD, 4006, Australia.
*E-mail addresses:* k.gulati@uq.edu.au (K. Gulati), s.ivanovski@uq.edu.au (S. Ivanovski).
[1] AJ and TG contributed equally.

https://doi.org/10.1016/j.bioactmat.2021.10.010
Received 23 June 2021; Received in revised form 22 August 2021; Accepted 6 October 2021
Available online 5 November 2021

the bio-inertness and non-resorbable nature of this oxide layer makes Zr an ideal candidate for dental implants. For dental implants, the ivory colour of $ZrO_2$, which resembles the natural tooth, makes it an aesthetic choice for dental restorations [19,20]. Various *in vitro* and *in vivo* investigations have established the biocompatibility and osteogenic potential of Zr-based implants [14]. However, in compromised patient conditions (inadequate bone quality/quantity, aged and diabetic patients), early establishment and long-term maintenance of osseointegration at the bone-implant interface, and soft-tissue integration at the transmucosal region of dental implants, may be inadequate [21].

Further, compromised conditions increase the possibility of bacterial infection and implant failure, requiring thorough decontamination and revision surgery [22,23]. Studies have shown that $ZrO_2$ surfaces are associated with reduced bacterial accumulation and that the bacterial plaque grown on $ZrO_2$ were less mature than Ti counterparts [24,25]. Additionally, $ZrO_2$ implants demonstrate reduced amounts of inflammatory infiltrate (albeit further clinical evidence is warranted) and promote soft-tissue integration [7]. This evidence suggests that $ZrO_2$ implants/abutments with low bacterial colonization potential and immunomodulatory properties may reduce the risk of peri-implant chronic inflammation associated diseases (such as mucositis and peri-implantitis). Hence, $ZrO_2$ may be particularly favourable for use in compromised conditions that predispose to peri-implant disease, including diabetic and immuno-compromised patients (eg. post-radiation therapy).

To address such challenges, surface modification of Zr-based implants to enable enhanced bioactivity and local therapy has been proposed to counter poor implant integration and bacterial infection. Moreover, attainment of immuno-modulation can further support integration and control of infection [26]. However, with various modification strategies employed, involving physical, chemical, and biological enhancements spanning across the macro-, micro-, and nano-scales, there is a gap in understanding the bioactivity and therapeutic effectiveness of such implant surface modifications. In this review, we compare and contraste the current knowledge of Zr-implant modification for improved understanding towards the clinical translation of the next generation of highly bioactive and therapeutic Zr implants.

## 2. Surface modification strategies and bioactivity evaluation

To date, various strategies have been employed to alter the surface texture of Zr-based implants; for example, physical, chemical, electrochemical and bioactive treatments. This review addresses a knowledge gap regarding surface modification of Zr implants to provide an improved understanding of the various strategies, their optimization, and effectiveness to enable easy clinical translation. Fig. 1 summarizes the various topographical, chemical and bioactive modifications performed on Zr implants to impart unique characteristics.

The interface between living tissue and the biomaterial surface has been studied extensively for Ti and its alloys [27] but remains poorly understood for Zr-based implants. Both the topography and chemistry of the implant surface influence early-stage cellular interaction and dictate the fate of the implant [28]. Studies have shown that $ZrO_2$ reduces bacterial adhesion and biofilm formation [29], while thickening of the native $ZrO_2$ film (varies between 2 and 5 nm) may improve the barrier effect against corrosion [30]. Both *in vitro* and *in vivo* studies have established that $ZrO_2$ implants have superior osseointegrating abilities [31]. Despite such favourable outcomes, it is noteworthy that the long-term clinical results have not been appropriately explored, and controversy regarding the osseointegration ability of $ZrO_2$ implants remain unaddressed [32].

In order to achieve successful long-term treatment outcomes for Zr-based orthopaedic and dental implants, modification to alter surface chemistry, topography, and bioactivity has been suggested, as widely applied for Ti implants [21,33]. Zr surface modification can influence cellular adhesion, proliferation, spreading morphology and differentiation of cells that interact with the implant at the implant-tissue interface [34]. For dental implants, such modifications can augment biocompatibility and integration (both hard- and soft-tissue) towards achieving favourable clinical outcomes and peri-implant stability.

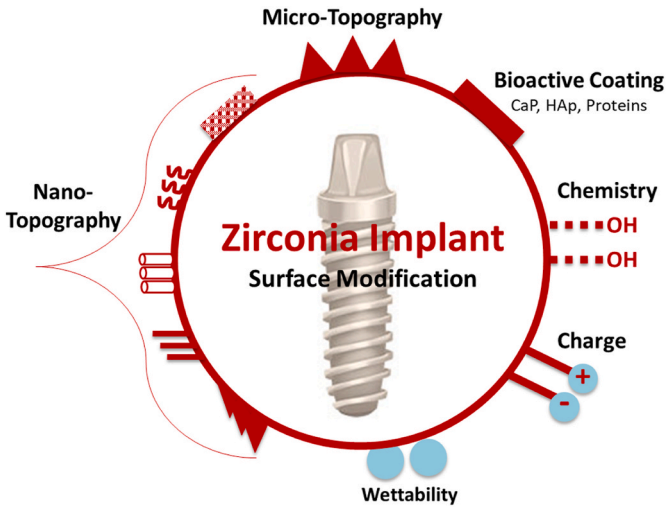


**Fig. 1.** Surface modification of Zirconia implants. Schematic representation of various surface topographical, bioactive and chemical modifications and the nano-engineered topographies.

### 2.1. Physical modifications

Physical or mechanical methods have been widely applied to fabricate rough or smooth implant surfaces via either subtraction or attrition processes. This serves the purpose of attaining desired surface topography towards bioactivity enhancements while also facilitating surface cleaning. Techniques like machining, polishing and grit-blasting have been applied towards the modification of Zr-based implants. Additionally, sputtering, plasma spraying, arc melting, physical vapour deposition, laser treatment and magnetron sputtering have also been performed to render Zr surfaces bioactive, as demonstrated in various investigations [35–40].

Initial attempts at modifying Zr implants involved grit blasting (alumina particles 50–110 μm), which enabled augmented peri-implant osteogenesis and osseointegration compared to machined Ti [41]. Studies have, however, shown that grit blasting can reduce fatigue resistance of $ZrO_2$ [42]. It has been suggested that the use of soft and round particles for grit blasting can reduce the formation of micro-cracks while still producing the desired roughness. Compared to machined, plasma-sprayed, and alumina blasted Ti, Zr sandblasted Ti implants significantly enhanced bone ingrowth, as demonstrated in sheep implantation *in vivo* [41].

Lasers have also been employed to modify the surface texture of $ZrO_2$ implants [43,44]. This method reduces the water contact angle (making the surface more hydrophilic), thereby augmenting the implants' osteogenic potential [44]. For instance, continuous-wave Nd: YAG laser-treated Zr oxidation on Ti was reported to enhance cell-material interactions *in vitro* [40]. It is noteworthy that laser-oxidized Zr has two orders of magnitude reduced wear rates compared to as-deposited Zr, attributed to the high surface energy and wettability [40]. Laser-oxidized Zr contains both monoclinic (m) and tetragonal (t) oxides, and increasing the t-phase (enhanced surface energy and hydrophilicity) has been shown to promote osteoblast functions [40]. Further, femtosecond laser exposure has been used to generate micro-grooves on $ZrO_2$, which increased the number of transverse collagen fibres and enhanced bone remodelling, compared with grit-blasted $ZrO_2$ and micro rough sand blasted and acid-etched (SLA)-Ti [45].

Plasma treated Zr surfaces have been generated using plasma electrolytic oxidation (PEO), plasma immersion ion implantation (PIII), ion-assisted arc-plasma deposition and simple plasma spraying [38,46–48]. Ivanova et al. reported the use of ion-assisted arc-plasma deposition on Ti–Zr alloys. They reported an increase in nanohardness due to increased Zr content in the coating [48]. Briefly, plasma-modified bare Zr, Zr coated Ti, or Zr incorporated Ti alloys have demonstrated enhanced osteogenic potential, superior mechanical properties and corrosion resistance [47,49]. Recently, Liu et al. reported deposition of Zr-incorporated amorphous carbon gradient multilayer films on Ti alloys via magnetron sputtering toward enhancing bioactivity, as well as mechanical and bio-tribological properties [50]. Compared to bare amorphous carbon and Ti alloy, the Zr–C/Ti alloys significantly augmented wear resistance and osteoblast functions (viability, proliferation and adhesion) *in vitro*. Yuan et al. fabricated a barrier layer of $ZrO_2$ nanofilm on Zn–Li alloys using atomic layer deposition (ALD) that enabled controlled biodegradation and augmented osseointegration abilities *in vivo* [51]. Noting that the release of metallic particles from the implant surfaces can trigger immuno-toxicity [52], the authors reported reduced $ZrO_2$ accumulation in organs, which was attributed to nanocoating, and suggested the use of $ZrO_2$ coating via ALD modification to control the corrosion of biodegradable metals and augment their biocompatibility. Various physical surface modifications of $ZrO_2$ and Zr alloys are summarized in Table 1.

### 2.2. Chemical modifications

Chemical immobilization or functionalization can further enhance the bioactivity of Zr implants, and as a result, acid-etching of implants has been widely explored and clinically applied. Further, dual topographical and chemical modifications and sol-gel methods have also been applied on Zr implants. For instance, grit-blasted Zr has been chemically treated with KOH, NaOH, and HF to enhance its bone-forming ability further. It has been reported that incorporation of fluoride on $ZrO_2$ resulted in bone-implant contact (BIC) of 81% [53]. Acid etching has been widely explored for both Ti- and Zr-based implants. Studies have shown similar osseointegration for acid-etched Ti and $ZrO_2$ implants, with no statistical difference observed [54]. It is noteworthy that dual micro- and nano-topography of acid-etched $ZrO_2$ implants may have a synergistic effect on biocompatibility and osseointegration [55]. It is also well established that micro and nanoscale modification can mechanically stimulate cells, thereby altering cell motility, adhesion and shape. This, in turn, influences the early establishment of osseointegration on dental implants [56].

Further, any differences in the physical and chemical characteristics of the implant (which are often interdependent and occur during implant surface modification) can significantly influence cellular responses (both host cells and pathogens). Another study reported a statistically significant reduction in three-species biofilm thickness on grit blasted and acid-etched $ZrO_2$ ($ZrO_2$-SLA) compared to Ti-SLA [57]. Further, beyond minor topographical differences, varied biofilm responses between modified Zr and Ti can also be attributed to material composition and hydrophilicity differences between metal (Ti) and ceramic ($ZrO_2$).

Other investigations involving chemical treatment of $ZrO_2$ include the use of various acids (HF, acetic and citric acids) [58], evaluation of the effect of concentration/time of HF treatment on $ZrO_2$ [59], testing osteoblast functions *in vitro* [60], and their comparison with established Ti counterparts [61]. Hempel et al. studied the response of osteoblast-like SAOS-2 cells on sandblasted, sandblasted/etched $ZrO_2$ and sandblasted/etched Ti and reported the pronounced effect of $ZrO_2$ on cellular adhesion, proliferation and differentiation [62]. Interestingly, both $ZrO_2$ modifications resulted in similar effects, and the difference with Ti was attributed to the difference in materials.

In terms of mechanical characteristics, a combination of heat and acid treatment can reduce $ZrO_2$ flexural strength due to monoclinic phase transformation and low-temperature degradation conditions [63]. Further, mechanical properties like flexural strength and hardness (altered by chemical treatment) can influence clinical performance.

Recently, He et al. studied the cytotoxicity of HF-treated Ti and Zr implants in a mini pig maxilla model *in vivo* [64]. Ti/Zr release was quantified using inductively coupled plasma optical emission spectrometry (ICP-OES) and inductively coupled plasma mass spectrometry (ICP-MS). At the same time, a histological analysis was performed 12 weeks post-implantation. Interestingly, Ti particle release from Ti implants was two times higher than Zr release from $ZrO_2$ implants, confirming reduced cytotoxicity and DNA damage from $ZrO_2$. Further, the sol-gel method has been used to modify HF-etched Ti implants with $ZrO_2$–$SiO_2$ sol, which did not alter Ti biocompatibility, and offered corrosion protection [65]. Next, machined cp Ti discs were dip-coated with either $TiO_2$ or $ZrO_2$ nanocoating, which upregulated bone-implant contact and removal torque values [66]. Bioactivity assessments of various chemically modified $ZrO_2$ implants are summarized in Table 2.

### 2.3. Electro-chemical modifications

Electrochemical techniques such as electrochemical anodization (EA) have been extensively applied to enable the fabrication of controlled metal oxide nanostructures, especially for Ti-based implants [21,67,68]. Briefly, EA involves immersion of target substrate (metal) as anode and non-target metal as a cathode in an electrolyte containing water and fluoride, connected via a DC power supply [69]. Under optimum conditions, controlled metal oxide nanostructures (metal oxide nanotubes or nanopores) are formed on the surface of the metal substrate (anode) [70]. Compared to alternate nano-engineering approaches, EA stands out due to its cost-effectiveness, scalability, and control over the physical/chemical characteristics of the fabricated nanostructures [71]. The same technique has been extended to fabricate $ZrO_2$ nanotubes/nanopores on the surface of Zr implants [72–79] (Table 3). Key findings from these studies include:

- $ZrO_2$ nanotubes improve the stability of Zr, and the corrosion resistance can be enhanced upon annealing of the nanotubes [80].
- Attempts at optimizing anodization to understand the growth of nanotubes on Zr [73].
- Fabrication of smooth and high aspect ratio nanotubes [77].

In 2017, Katunar et al. reported an extensive study focussed on *in vitro* and *in vivo* bioactivity evaluation of anodized Zr implants [81]. Cp Zr cylinders were anodized at 30 and 60 V for 60 min, followed by mechanical preparation and degreasing. *In vitro* culture of mouse myoblasts C2C12-GFP, osteoblastic MC3T3-E1 cells and the macrophage RAW 264.7 murine cells revealed increased cell spreading and osteoblastic and osteoclastic morphology. Further, *in vivo* implantation in a rat femur osteotomy model confirmed new bone formation around 60 V anodized Zr implants. In a similar study, 60 V anodized Zr implanted in a rat model *in vivo* obtained significantly enhanced cancellous bone volume and trabecular thickness, confirming the earlier onset of osseointegration around anodized implants [82].

By tuning anodization conditions, controlled nanotopographies can be fabricated on Zr implants. We have recently demonstrated the fabrication of nanopores and nanotubes on micro-rough Zr wires, mimicking clinically utilized Zr implants and demonstrating clinical translation of anodized nano-engineered Zr implants [78]. We have also shown that dual micro-nano structures can be fabricated by conserving the underlying micro-rough topography of Zr implants and superimposing nanotopography [79]. Frandsen et al. compared the bioactivity of $ZrO_2$ nanotube modified Zr implants and bare Zr implants using osteoblasts *in vitro* and reported enhanced initial adhesion and spreading on nanotubes, along with highly organized cytoskeleton, increased ALP activity and mineralization [83]. Further, annealing $ZrO_2$ nanotubes

**Table 1**
Summary of surface modification of Zr/$ZrO_2$ or Zr-alloyed implants via physical methods.

| No. | Surface | Modification Strategy | Treatment | Dimensions | *In-vivo/In-vitro* studies | Bioactivity Evaluation/Conclusion | Ref. |
|---|---|---|---|---|---|---|---|
| 1 | Cp Zr | Mechanical polishing + femtosecond laser-assisted texturing | Smooth polished surface | D: 10 mm<br>T: 2 mm | *In-vitro* HDFa (Human Dermal Fibroblasts-Adult) cells) and *in-vivo* (rat) model | Similar to Ti alloy, modified Zr bioactivity depends on both topography and chemistry | [35] |
| 2 | Zr plate | Particle blasting | Zr Macro -machined<br>Zr Micro - particle blasting | D: 6 mm<br>T: 1 mm | *S. epidermidis* | High roughness and hydrophilicity increase bacterial interaction with surfaces. | [89] |
| 3 | Zr oxide discs | Cell cultured directly on Zr oxide discs | Expression profiling by DNA microarray | – | Osteoblast-like cells (MG-63) *in vitro* | $ZrO_2$ is able to modulate immunity, vesicular transport and cell cycle regulation | [3] |
| 4 | Zr | Physical treatment | Machined Ti<br>Titanium oxide: plasma sprayed<br>Alumina sandblasted<br>Zr: sandblasting | – | Sheep tibia mid-diaphysis cortical bone *in vivo* | Zr-SL implants showed significantly increased bone ingrowth and microhardness than Ti. | [90] |
| 5 | $ZrO_2$ | wTo different glass layers: AP40<br>RKKP | Ball milling | – | SBF | Both glass coatings substantially enhanced $ZrO_2$ integration with bone cells | [91] |
| 6 | $ZrO_2$ | – | Magnetron sputtering deposition | – | *E. coli* and *S. aureus* | *S. aureus* adhesion was lower on $ZrO_2$ | [36] |
| 7 | Zr5Ti (5 Ti wt%)<br>Zr25Ti (25 Ti wt%)<br>Zr45Ti (45 Ti wt%) | HAP-$ZrO_2$-Ag | Multiple electron beam drip melting + plasma laser deposition | D: 8 mm<br>H: 8 mm | Pig tibia model *in vivo* | Significantly augmented osseointegration for HAP-$ZrO_2$-Ag coated Zr45Ti | [5] |
| 8 | Zr Macro<br><br>Zr Micro | – | Machined: only cleaned<br>Particle Blasting: airborne particle abrasion with 50–100 μm $Al_2O_3$ particles. | T: 1 mm<br>D: 6 mm | *S. epidermidis* | Machined samples showed reduced biofilm formation | [93] |
| 9 | Ti–13Nb–13Zr | – | Plasma electrolytic oxidation (PEO) | – | SBF and human bone marrow-derived mesenchymal stem cells (hBMSCs) *in vitro* | Upregulated osteoblast activity | [38] |
| 10 | Ti–35Nb–7Zr–5Ta (β micro-structure) | – | Machined<br><br>Plasma electrolytic oxidation | – | – | Lowest hardness and elastic modulus ($p < 0.05$) and increased polarisation resistance relative to cpTi.<br>Porous surface with increased roughness, surface free energy, hardness and electrochemical stability | [94] |
| 11 | Ti6Al4V | Ti–Nb–Zr–Si thin film metallic glass (TFMG) | Sputtering | – | Cytotoxicity test with L929 fibroblast cells | Superior corrosion resistance and electrochemical stability, non-cytotoxicity, better hemocompatibility | [95] |
| 12 | TiZr alloy | – | MAO treatment | – | MG-63 cells and SKF cells | Increase in cell viability and cell growth | [96] |
| 13 | Ti–25Nb–3Mo–3Zr–2Sn | Without the α phase<br>With α phase | Surface mechanical attrition treatment (SMAT) | – | hFOB1.19 | Enhanced the osteoblast response | [97] |
| 14 | (Y,Nb)-TZP/alumina | – | Cold isostatic pressed | – | HOS cells | Supports continuous cellular growth | [98] |
| 15 | HA- $ZrO_2$ composite | Ti6Al4V alloy | Magnetic sputtering | – | – | The growth of bone tissue reduce its residual stress | [99] |
| 16 | Ti–35Nb–10Zr | HA thin film coating | Femtosecond laser texturing | – | MG 63 osteoblast-like cells *in vitro* | Significantly higher cell attachment and spreading | [100] |
| 17 | Ti–35Nb–2Ta–3Zr | – | Micro-arc oxidation | – | – | Excellent corrosion resistance and hydrophilicity | [101] |
| 18 | Zr and $ZrO_2$ alloyed layers | 316 L stainless steel | Plasma surface alloying + annealing | – | MC3T3-E1 preosteoblast cells *in vitro* | Significantly enhanced the wear resistance, improved adhesion and spreading | [102] |
| 19 | Zircaloy-2 alloy | Potassium hydroxide/sodium silicate electrolytes | Plasma electrolytic oxidation | – | – | Enhanced corrosion resistance | [103] |
| 20 | Ti15Zr alloy | – | Plasma electrolytic oxidation (PEO) | D: 15 mm<br>T: 1 mm | Bacterial test: *S. sanguinis*<br>Protein adsorption: Albumin | Improved albumin adsorption, reduced bacterial adhesion, improved hardness, roughness and corrosion resistance | [104] |
| 21 | Pure Zr | Ti | Continuous-wave Nd: YAG laser | T:7 μm | Human osteoblasts *in vitro* | Enhanced biocompatibility, excellent cell-material interactions | [40] |
| 22 | Zr incorporated amorphous carbon | Ti alloys | Magnetron sputtering | – | Immortalized calvarium osteoblast-like cells *in vitro* | Improved biocompatibility | [50] |

(*continued on next page*)

**Table 1** (*continued*)

| No. | Surface | Modification Strategy | Treatment | Dimensions | *In-vivo/In-vitro* studies | Bioactivity Evaluation/Conclusion | Ref. |
|---|---|---|---|---|---|---|---|
| 23 | Zr | Ti | Ion-Assisted Arc-Plasma Deposition in Vacuum | – | – | Reduced elastic modulus, enhanced elastic strain to failure and plastic deformation resistance | [105] |
| 24 | $ZrO_2$ | WE43 Mg | Liquid Phase Plasma Technique | | SBF *in vitro* | Enhanced cell proliferation and differentiation | [106] |
| 25 | Zr | AZ91 Mg alloys | Plasma Immersion Ion Implantation (PIII) | T: 80 nm | MG-63 cells *in vitro* | Enhanced corrosion resistance, improved antimicrobial properties *in vitro,* promoted the bone formation | [47] |
| 26 | $ZrO_2$ | Zn-0.1 (wt.%) Li alloy | Atomic Layer Deposition (ALD) | – | Mouse osteoblast-like cells (MC3T3-E1) *in vitro*. Ten-week old male Sprague-Dawley (SD) rats *in vivo* | Improved cell adhesion and viability *in vitro*. Promoted osseointegration and controlled biodegradation behaviour *in vivo*. | [107] |
| 27 | Zr | - | Plasma electrolytic oxidation | – | Human osteosarcoma cells *in vitro* | Porosity increased with frequency, superior pitting/corrosion resistance, good apatite forming ability, and cell adhesion | [108] |

increased corrosion resistance compared to bare Zr and as formed $ZrO_2$ nanotubes [80]. It is worth noting that the hydrophilicity of $ZrO_2$ nanotube surfaces increases with reduced diameters and annealing (which results in surface cracks), while hydrophilicity reduces with ageing (when nanotubes were exposed to air for 105 days) [84]. These were attributed to the balance of capillary force and reduction in hydroxyl content. Compared with anodized Ti with $TiO_2$ nanotubes, similar results are seen with respect to annealing (increased hydrophilicity) and ageing (reduced hydrophilicity) [85]. However, for $TiO_2$ nanotubes, hydrophilicity decreases with reducing diameters [86]. It is notable that nanotube diameter can be increased via increasing the voltage, current or time of anodization [87,88]; however, we have recently reported that for fabrication of $ZrO_2$ nanotubes/nanopores on Zr, these approaches can result in cracks on the anodic film (when anodizing curved Zr substrates) [78] and excessive growth rates (which can result in nanograss like structures) [79].

### 2.4. Bioactive coatings

Bioactive coatings on $ZrO_2$ have been developed to augment osteoblast functions, induce hydroxyapatite formation, contribute to osteogenesis, and achieve antibacterial properties [92,115]. Numerous studies have reported bioactivity enhancements toward augmented osseointegration/soft-tissue integration on Zr implants [4,129,142–146] involving modifications with calcium phosphate (CaP), hydroxyapatite (HA), and various biopolymers and biomacromolecules [142,146–149]. Bioactivity enhancements using hydroxyapatite and calcium are presented in Table 4.

#### 2.4.1. Calcium phosphate (CaP) coatings

CaP is a critical mineral component of bone, and incorporation of CaP into implants can lead to the rapid establishment of bone-implant integration [149,150]. CaP coatings enhance calcium deposition and protein adhesion on Zr-based implants, improving surface bioactivity [129,151]. Stefanic et al. reported a stabilized beta-tricalcium phosphate (β-TCP) layer on $ZrO_2$ implants via chemical deposition and hydrothermal treatment (900 °C) [151]. Such β-TCP coatings enhanced the *in vitro* apatite deposition in simulated body fluid (SBF) solution and promoted serum protein adhesion to $ZrO_2$ substrates [151]. In another study, Quan et al. synthesized and coated a $ZrO_2$–CaP composite onto $ZrO_2$ substrates via chemical co-precipitation and significantly enhanced the *in vitro* expression of alkaline phosphatase (ALP), interleukin-6 (IL-6), and transforming growth factor-β (TGF-β) in murine calvaria osteoblasts [129].

It is noteworthy that CaP coatings have weak bonding strength with $Zr/ZrO_2$ substrates, especially those obtained from the physical deposition method. Consequently, multiple attempts have been made to reinforce its adhesive strength on implants, including co-coating with HA, laser treatment (before CaP), and hydrothermal sintering (after CaP) [142,149,152]. Besides these techniques, the multiple-layer composite coating is an alternative to obtain stable CaP coatings, as reported by Bao et al. [153]. In this method, a thin $TiO_2$ film is deposited and immobilized on Zr substrate by sol-gel technique and annealing, followed by the sequential deposition and superimposition of octacalcium phosphate (OCP) composite onto the $TiO_2$ film in Si-OCP solutions [153]. Such sequential deposition can generate a consistent Si-doped OCP coating layer without cracks/defects, and the reliable mechanical stability of such coating has been confirmed by ageing tests [153]. Further, Stefanic et al. confirmed the formation of a stable CaP coating via two-step biomimetic deposition: an amorphous OCP layer was initially precipitated on $ZrO_2$ substrate and transformed into an apatite phase that served as a template for superimposing the final OCP coatings [154]. Such technique is scalable and reproducible and allows synthesizing a CaP layer that is strongly integrated onto Zr substrates [154].

#### 2.4.2. Hydroxyapatite (HA)

With a similar crystalline structure to dental enamel, dentin, and alveolar bone, hydroxyapatite (HA) has been used to augment osteogenic potential at bone defect sites [144,155]. Compared with other biological coatings on $Zr/ZrO_2$, HA-based coatings have been widely applied in various *in vitro* and *in vivo* investigations to achieve bioactivity enhancements [5,147,156,157]. Applying thermal treatment to Zn-doped hydroxyapatite (ZnHA)-coated $ZrO_2$ substrate (1200 °C for 2 h, after coating) may convert part of the ZnHA coating into other crystalline forms, such as β-calcium phosphate (β-TCP), calcium oxide phosphate, and calcium zirconium oxide, to stabilize the coating layer [156]. Such modified ZnHA coatings have favourable mechanical properties and are firmly adhered to the underlying $ZrO_2$ substrate. ZnHA has shown improvements with respect to osteogenic potential by enhancing MC3T3-E1 osteoprogenitor cell proliferation and spreading morphology *in vitro* [156]. Cho et al. reported significantly enhanced expression of ALP, alizarin red, and bone marker genes in MC3T3-E1 cells *in vitro*, using aerosol deposited HA coating [147]. Histological findings from *in vivo* studies have reported osteogenic enhancements of HA-coated $Zr/ZrO_2$ [5,157].

Various strategies have been employed to modify $Zr/ZrO_2$ with HA. After coating different Zr alloys with HA via plasma laser deposition, Trinca et al. implanted HA-Zr implants in the tibial crest of minipigs and assessed bone formation at different distances from the implants [5]. Briefly, superior new bone formation was observed around HA-coated Zr implant surfaces within one month, with numerous infiltrating cuboid-shaped osteoblasts [5]. Moreover, there were fewer infiltrating macrophages around HA-coated implants than the non-coated Zr counterparts (Fig. 2) [5]. In another *in vivo* study, nano-crystallized

**Table 2**
Chemical modification of Zr/$ZrO_2$ and Ti–Zr alloys towards bioactivity enhancement.

| No. | Surface | Modification Strategy | Treatment | Dimensions | *In-vivo/In-vitro* studies | Bioactivity Evaluation/Conclusion | Ref. |
|---|---|---|---|---|---|---|---|
| 1 | Cylindrical low-pressure injection moulded $ZrO_2$ | Chemical treatment, acid-etched | Ti-SLA controls | Threaded implants with a 6-cornered shaft<br>D: 4.1 mm<br>L: 10 mm | Mini pig maxillae *in vivo* | Leached $ZrO_2$-NPs showed lower cytotoxicity and DNA damage compared to Ti-NPs in human cells. No difference in osseointegration between $ZrO_2$ implants and Ti-SLA controls regarding peri-implant bone density and BIC ratio. | [109, 110] |
| 2 | 3Y-TZP | Physical and chemical treatment | Micro-structured Ti | D: 5 mm | *In-vitro* Primary human bone cells (HBC) advanced osseointegration model | $ZrO_2$ surface showed increased fibrinogen adsorption, platelet adhesion, activation, and thrombogenicity compared to Ti surfaces. Mineralization of HBC was significantly higher on $ZrO_2$ but significantly lower compared to nanostructured Ti. | [111] |
| 3 | Zr | Treated by calcium phosphate slurry | – | – | SBF *in vitro* | Calcification of an osteoblast-like cell was enhanced on the treated surface | [112] |
| 4 | Zr | Varied concentrations of phosphate, silicate and KOH based electrolyte using a pulsed DC power source | Plasma electrolytic oxidation (PEO) | T: 6–11 μm | Human osteosarcoma cells *in vitro* | Cells firmly adhered and spread on all the oxide films. Silicon doped films showed higher surface roughness and wettability. | [113] |
| 5 | Ti–5Zr<br>Ti–10Zr<br>Ti–15Zr | – | Machined polished (MP)<br>Machined polished + double acid etching (MP-DAE) | D: 10 mm<br>T: 2 mm | MC3T3-E1 osteoblasts *in vitro* | MP-DAE treatment improved mechanical properties, cell adhesion/proliferation, and corrosion resistance. | [114] |
| 6 | TiZr | – | Polished (P)<br>Polished hydride (PH)<br>Polished, HNO3/HF acid-etched and hydride (PEFH)<br>Machined (M)<br>Machined hydrides (MH)<br>Machined, HNO3/HF acid-etched and hydride (MEFH)<br>Machined and HCL/H2SO4 acid-etched (MES)<br>Machined, HCL/H2SO4 acid-etched and hydride (MESH) | D: 4.39 mm<br>T: 2 mm | Primary human gingival fibroblasts *in vitro* | Increased expression of fibrotic markers<br>Decreased expression of fibrotic markers<br>–<br>Cell alignment<br>Increased initial cell attachment and the expression of genes necessary responsible for a collagen-rich ECM<br>–<br>–<br>– | [116] |
| 7 | $ZrO_2$ | ORMOSILs (Organically Modified Silicate) | Sol-gel process | – | Human osteoblast cell line MG-63 (CRL-1427) *in vitro* | Supports cell adhesion and proliferation. | [117] |
| 8 | $ZrO_2$ | cpTi | Sol-gel Technique | – | *In vivo* in rat tibiae | Improved differentiation of rat MSCs into osteoblasts, increased bone-to-implant contact and removal torque values | [118] |
| 9 | $ZrO_2$<br>$ZrO_2$–$SiO_2$ | Ti | Sol-gel | – | Human osteoblasts and artificial saliva *in vitro* | Reduced Ti susceptibility to corrosion | [119] |

HA-coated $ZrO_2$ implants were implanted into the jaws of Beagle dogs, and histological findings confirmed significantly enhanced new bone formation around coated implants (33 ± 14%) after six weeks in comparison with the non-coated controls (21 ± 11%) [157].

It is noteworthy that HA modified Zr/$ZrO_2$ implants may cause detachment/delamination of HA coatings when facing high torque at the implant-bone interface during implant placement. Thus, many studies have focused on enhancing HA coatings' bonding stability on Zr/$ZrO_2$ substrates [142,143,145]. One strategy is ceramic slurry infiltration treatment before coating, forming a porous layer on $ZrO_2$ substrate, as reported by Miao et al. [155]. Such a porous layer increases the HA-$ZrO_2$ contact area resulting in higher interfacial bonding strength [155]. An alternative approach involves coating combined yttria-stabilized $ZrO_2$ (Y-TZP) powder with HA crystals on $ZrO_2$ substrates, resulting in significantly increased adhesion strength on $ZrO_2$ surface compared to bare HA coatings [145]. Such composite coatings enhanced human osteoblasts (HOBs) proliferation and ALP secretion *in vitro* [145]. Further, applying a 2-step freeze-drying treatment (−40 °C for 4 h at 89 μBar, followed by room temperature drying for 24 h at 23 μBar) resulted in a stable HA coating layer on microporous $ZrO_2$ substrates with favourable compressive and flexural strength [143].

It is noteworthy that HA in the bulk form possesses inadequate mechanical characteristics, including weak bending stress and low fatigue resistance [158]. Further, the mismatched thermal expansion between

**Table 3**
Summary of electrochemical techniques utilized to achieve enhanced bioactivity from $Zr/ZrO_2$ implants.

| No. | Surface | Modification Strategy | Treatment | Dimensions | *In-vivo/In-vitro* studies | Bioactivity Evaluation/Conclusion | Ref. |
|---|---|---|---|---|---|---|---|
| 1 | Cp Zr cylinders | Mechanical polishing + anodization | As- received | L: 40–50 mm<br>D: 1 mm | Twelve-week-old male WKAH/Hok rats *in vivo* | Anodized implants at (60 V) augments osseointegration | [120] |
| 2 | Cp Zr cylinders | Mechanical polishing + anodization | As- received<br>Anodized:30 V (Zr30 V)<br>Anodized:30 V (Zr60 V) | L: 40–50 mm<br>D: 1 mm For *in-vitro* 1 $cm^2$ plates | *In-vivo*: rat femur osteotomy model.<br>*In-vitro*: RAW 264.7 for osteoclast differentiation, pre-myoblast C2C12-GFP and preosteoblastic MC3T3-E1 cells | Anodized Zr allows bone augmented cell adhesion and proliferation, affecting cytoskeleton alignment and permitting bone cell differentiation. Zr60 V enabled accelerated bone formation. | [121] |
| 3 | Zr | Two-step anodization | Zr flat<br>Zr NT (Nanotubes) | – | MC3T3-E1 mouse osteoblast cells *in vitro* | Increased cell adhesion, spreading, ALP activity and mineralization for ZrNT. | [83] |
| 4 | Zr | Anodization | Zr NT | – | – | Reduced hydrophilicity with reducing diameters | [84] |
| 5 | $ZrO_2$ | Anodization | Annealed | – | SBF | Reduced corrosion resistance for annealed $ZrO_2$ | [80] |
| 6 | Zr-2.5Nb | – | EA | – | SBF | Enhanced corrosion resistance | [122] |
| 7 | $TiO_2$–$ZrO_2$–$ZrTiO_4$ (20 V)<br>$TiO_2$–$ZrO_2$–$ZrTiO_4$ (25 V)<br>$TiO_2$–$ZrO_2$–$ZrTiO_4$ (30 V)<br>$TiO_2$–$ZrO_2$–$ZrTiO_4$ (35 V) | – | Anodization + annealing | D: 40 ± 12 nm<br>D: 59 ± 17 nm<br>D: 64 ± 23 nm<br>D: 82 ± 26 nm | SaOS2 cells *in vitro* | 40 nm diameter nanotubes had the highest percentage of cell adhesion | [123] |
| 8 | ZrTi alloy | – | Electrodeposition + thermal treatment | – | MC3T3-E1 osteoblasts | Good viability decreased ROS level and a better cytoskeleton organization | [124] |
| 9 | $ZrO_2$ | $TiO_2$ | Anodic Plasma-Electrochemical Oxidation | – | Primary human osteoblast cells, bone sialoprotein (BSP) and osteocalcin (OC) *in vitro* | Upregulated proliferation and bone formation ability | [125] |

HA and Zr and decomposition of HA during sintering can limit the mechanical bonding strength of HA coatings on Zr substrates [155]. This can result in mechanical brittleness and weakness of the HA-coated Zr implants, compromising the safe implantation and functioning of HA modified $ZrO_2$ implants. To address this, Faria et al. fabricated a $ZrO_2$-HA/TCP composite coating using gas compacting and sintering techniques to produce superior mechanical stability with enhanced hydrophilicity [142]. Table 5 summarizes the bioactivity enhancements on yttria-stabilized zirconia (YSZ) implants using Silica, HA, $TiO_2$ and Si3N4 particles.

### 2.4.3. Dopamine and poly-dopamine

Dopamine and poly-dopamine (PD) can aid in cell-material adhesion and interaction, and their use as coatings has been proposed to augment bioactivity of $Zr/ZrO_2$ surface [148]. Dopamine coating can improve cell adhesion by influencing cell filopodia and enhancing protein adsorption on modified $Zr/ZrO_2$ implants [148,164,165]. Compared with HA and CaP coatings, dopamine coating on $Zr/ZrO_2$ can be achieved via physical deposition (immersion) in dopamine hydrochloride solution [164], although to obtain evenly distributed dopamine coatings, it is necessary to maintain constant stirring and temperature stabilization (37–50 °C) of the dopamine hydrochloride solution [164,165]. $ZrO_2$ substrates modified with 3,4-dihydroxy-L-phenylalanine (L-DOPA) coatings exhibit enhanced protein adhesion capacity and increased MG-63 human osteoblastic cell proliferation and cell spreading *in vitro* compared with uncoated $ZrO_2$ substrates [166]. Further, increased proliferation of human gingival fibroblasts (hGFs) on PD coated $ZrO_2$ *in vitro*, with enhanced expression of fibronectin, integrin β1, and secretion of collagen 1 has been reported [167]. Clearly, PD coated Zr implants can be used towards soft-tissue integration and osseointegration to ensure the long-term success of a dental implant system [167].

### 2.4.4. Biomacromolecular coatings

Biomacromolecules such as Arginylglycylaspartic acid (RGD), a minimal recognition sequence within fibronectin that can promote cell interactions, holds great promise in augmenting the bioactivity of conventional implants [168,169]. Since RGD coatings must be performed under mild conditions to prevent protein/peptide denaturation, sequential pre-treatments are required prior to its coating; these include acid etching, plasma treatment, and salinization [169]. As Fernandez-Garcia et al. reported, RGD-functionalized $ZrO_2$ implants increased murine osteoblasts MC3T3-E1 adhesion rates *in vitro* [169]. An alternative protocol for immobilizing RGD on $ZrO_2$ substrate is covalent bonding, which involves sequential immersion in acid/alkaline solutions to form hydroxyl groups leading to covalent bonding and strengthening of the RGD coating layer [170]. Such RGD-coated $ZrO_2$ surfaces have been reported to enhance proliferation, adhesion, and differentiation of MG-63 osteoblasts *in vitro* [170].

Protein and cytokine coating of implant surfaces is problematic due to potential denaturation during the immobilization process [168]. Thus, hydrothermal treatment, which can effectively immobilize CaP/HA coatings, is unsuitable for coating sensitive biomacromolecules [146]. Moreover, to obtain a stable biomacromolecule coat, $Zr/ZrO_2$ substrates must be pre-treated [146]. Aiming to enhance the efficiency of fibronectin (FN) coating on $ZrO_2$ implants, Rubinstein et al. utilized ion beam assisted deposition (IBAD) to create a nanostructured $ZrO_2$ surface (nano-peaks with negatively charged patches) [146]. The nanopeaks obtained by IBAD were ultra-hydrophilic and had enhanced FN adhesion capacity, thus promoting cell adhesion on the FN-coated $ZrO_2$ implant surface [146].

Bone morphogenetic protein-2 (BMP-2) and growth and differentiation factor-5 (GDF-5) have also been immobilized on $ZrO_2$ by applying multiple hydrogel loading treatments [4]. Briefly, the $ZrO_2$ surface was initially functionalized by 2-aminoethyl methacrylate (AEMA)-conjugated HA (HA-AEMA) and then immersed in a hyaluronic hydrogel that contained BMP-2 or GDF-5 [4]. The BMP-2 and GDF-5 loaded ZrO2 surface showed significantly enhanced alkaline phosphatase (ALP) activity from MG-63 osteoblasts at day 7 in a dose-dependent manner.

**Table 4**
Use of hydroxyapatite and calcium to augment bioactivity of $Zr/ZrO_2$ implants.

| Study | Surface | Modification Strategy | Treatments | Dimensions | *In-vivo/In-vitro* studies | Bioactivity Evaluation/Conclusion | Ref. |
|---|---|---|---|---|---|---|---|
| 1 | Zr | HAP-based bioceramic | Single-step Plasma Electrolytic Oxidation (PEO) | – | SBF *in vitro* | Enhanced bioactivity and reduced microbial adhesion | [126] |
| 2 | $ZrO_2$ | Ca-doped | Wet synthesis and self-assembly | – | *Saos-2* human osteoblastic cells *in vitro* | Increased stability and enhanced osteoblast activity. | [127] |
| 3 | Zr | CaO partially stabilized $ZrO_2$ (Ca-PSZ) coating covered with HA | Micro-arc oxidation (MAO) and hydrothermal treatment (HT) | Nanorods D:50 nm L:450 nm | – | Good hydrophilicity, excellent apatite-inducing ability | [128] |
| 4 | $ZrO_2$ | CaP decomposed from HAP during sintering | Chemical co-precipitation method | – | Rat osteoblast cells *in vitro* | Augmented tensile and binding strength. Enhanced proliferation and ALP activity. | [129] |
| 5 | $ZrO_2$ | Laminin-5 | Argon plasma | – | Epithelial cells | Enhanced cell adhesion | [130] |
| 6 | Zr | HAP-based plasma electrolytic oxide (PEO) | Single-step plasma electrolytic oxidation | – | *In vitro*: simulated body fluid (SBF), MTT assay and bacterial adhesion | PEO/Zr surface significantly improved bioactivity under SBF. Reduced bacterial adhesion on PEO/Zr | [131] |
| 7 | TiZr | – | Powder metallurgy followed by alkali-heat treatment and Ca-deposition | – | Osteoblast-like cells (SaOS2) | TiZr alloys exhibited excellent cytocompatibility and satisfactory bioactivity | [132] |
| 8 | ZrTi alloy | $HA/TiO_2$ | Sol-gel method | – | SBF | Good bone-like apatite forming | [133] |
| 9 | Ti–13Nb–13Zr alloy | Incorporation of Ca ions | Electropolishing + plasma electrolytic oxidation (PEO) | – | SBF, hBMSC | Enhanced bioactivity | [134] |
| 10 | $ZrO_2$/HA composite film | Zr | Plasma electrolytic oxidation coupled with electrophoretic deposition process in a single step | – | SBF, Human osteosarcoma cells | Human osteosarcoma cells could attach, adhere and propagate well | [135] |
| 11 | Ti–13Nb–13Zr (TNZ) | Anodization + Adsorbed collagen + Adsorbed lactoferrin | Plasma electrolytic oxidation coupled with a sol-gel process | – | Osteoblast-like MG-63 | Enhanced surface roughness and cytocompatibility | [136] |
| 12 | Ti–3Zr–2Sn–3Mo–25Nb | HA coating | Micro-arc oxidation (MAO) | – | Left proximal femoral medullary canal of beagles *in vivo* | Significantly promoted bone ingrowth and the mechanical performance of the bone-implant interface | [137] |
| 13 | Ti–35Nb–xZr alloy | HA coating | Electron beam-physical vapour deposition | – | – | Ti–35Nb–10Zr alloy showed higher corrosion potential. HA/Ti–35Nb–10Zr alloy showed high polarisation resistance by crystallization. | [138] |
| 14 | Ca doping $ZrO_2$ | NiTi alloys | Cathodic plasma electrolytic deposition (CPED) technology | – | SBF *in vitro* | Enhanced corrosion resistance, excellent apatite-inducing ability, enhanced bioactivity. | [139] |
| 15 | $ZrO_2$–$Y_2O_3$ $ZrO_2$–CaO | Mg–Ca Mg–Ca–Zr | Atmospheric Plasma Jet Technique | – | MTT cell viability | Higher polarisation resistance Improved cell adhesion and viability | [140] |
| 16 | Ca with Zr coating | – | Plasma spray technique | – | SBF, Osteoblast-like MG63 cells *in vitro* | Cytocompatibility and enhanced cell growth and proliferation | [141] |

NPs, nanoparticles; BIC, bone-implant contact; HA/HAP, hydroxyapatite; SBF, simulated body fluid.

Similarly, Alizarin Red staining showed increased calcium deposition *in vitro* from MG-63 cells on BMP-2, and GDF-5 coated Zr implants. mRNA expression for ALP and osteopontin in MG-63 cells *in vitro* was enhanced on GDF-5 and BMP-2 functionalized $ZrO_2$ surface, further indicating enhanced osteogenic potential (Fig. 3) [4].

### 2.5. Ultraviolet irradiation

Previous studies have established that UV-irradiated Ti surfaces exhibit increased bioactivity and osteoconductive properties [171]. The same strategy had been extended to $ZrO_2$ surfaces. In a pioneering study, Att et al. evaluated the effect of UV light exposure on $ZrO_2$ [1]. They employed a 15 W bactericidal lamp (250–360 nm) as the UV light source for a period of 48 h and observed an increase in hydrophilicity on the $ZrO_2$ surface (Fig. 4a). Enhanced cellular attachment, spread, and proliferation of bone marrow cells were also observed for $ZrO_2$ surfaces exposed to UV over this time. Although ALP activity and mineralization was significantly higher in UV treated samples, a significant difference in gene expression for osteogenic markers between treated and untreated surfaces was not achieved. This led to the conclusion that enhanced ALP activity was due to the higher number of cells attached to $ZrO_2$ surfaces upon UV treatment, indicating that UV treatment improved cell attachment and proliferation.

In another study, Tuna et al. evaluated the effect of UV treatment on two types of biomedical grade Zr, Zr1 [($ZrO_2$ 85.7 wt%; $Al_2O_3$ 8.3 wt%; $Y_2O_3$ 4.3 wt%; $La_2O_3$ 1.7 wt%] and Zr2 [$ZrO_2$ 93 wt%; $Y_2O_3$ 5 wt%; $HfO_2$ 1.9 wt%; $Al_2O$ 0.1 wt%] [172]. Smooth (m) and rough (r) $ZrO_2$ (roughened by sandblasting) were exposed to a 15 W bactericidal lamp (250–360 nm) for 48 h. Contact angle analysis showed a significant shift of surface properties from hydrophobic to hydrophilic upon UV treatment. UV treatment also reduced the amount of carbon present on the surface. Further, the culture of osteoblasts *in vitro* revealed accelerated attachment and enhanced spreading on the UV treated surfaces. However, no significant difference was observed in ALP activity due to

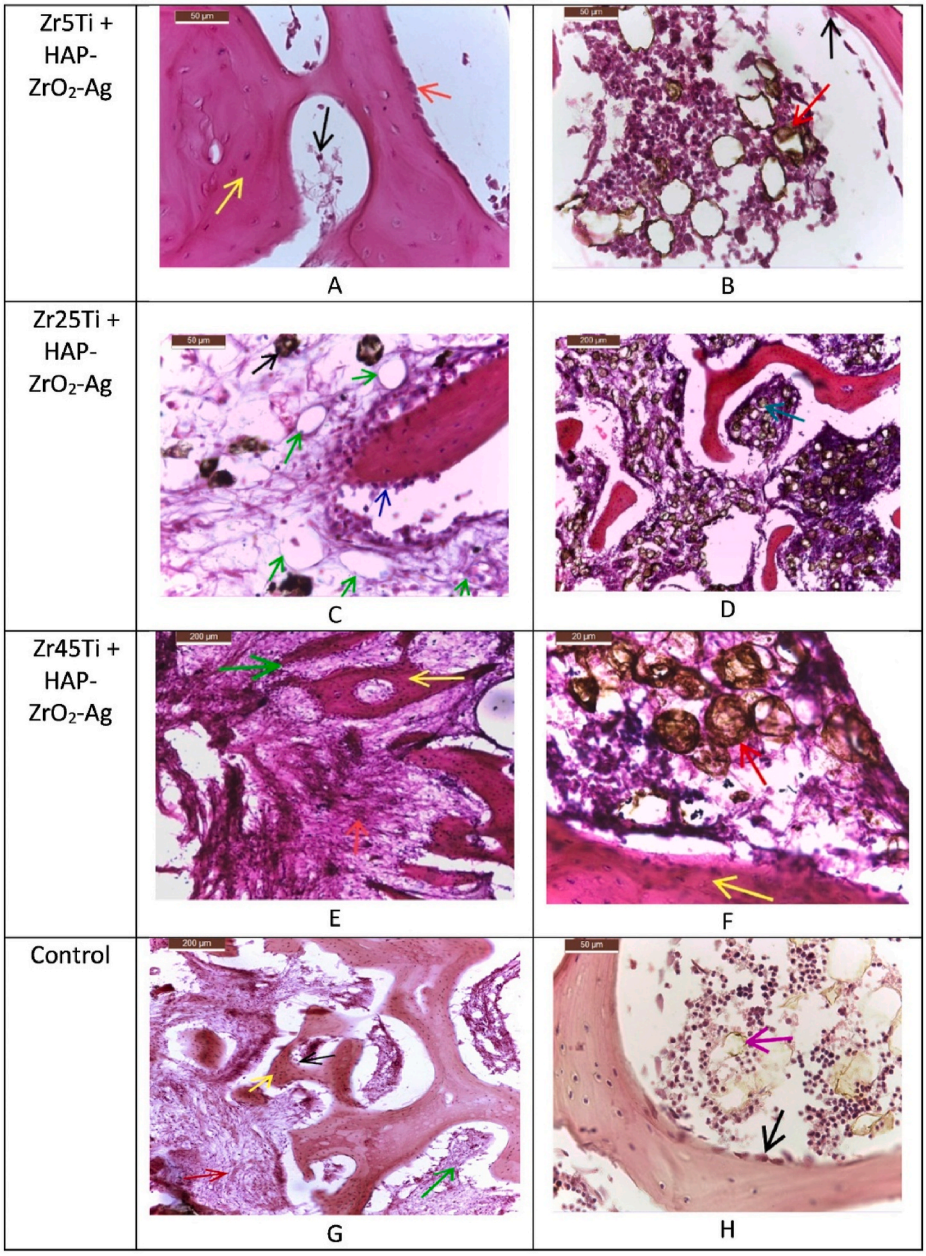


**Fig. 2.** ZrTi alloy implant modified with hydroxyapatite and silver. Histology of bone tissue at implant surfaces post-implantation in pig tibiae after one month. Bone tissue around ZrTi alloys coated with a composite of hydroxyapatite-zirconia-silver layer (HAP-$ZrO_2$-Ag; A-F) and uncoated ZrTi alloys (control group; G, H). (A, C, E, G) Bone area adjacent to the implant (<2500 μm); (B, D, F, H) bone area 2500–6000 μm to the implant surfaces. For all coated ZrTi implants, the newly generated bone (yellow arrows) was evident after one-month healing with numerous cuboid-shaped osteoblasts infiltration (red arrows and green arrows). Less bone formation was observed around non-coated ZrTi surface, with numerous macrophages infiltration (black arrows). Adapted with permission from Ref. [5].

**Table 5**
Surface modification of Yttria-stabilized Zirconia (YSZ).

| No. | YSZ/Calcia Coating | Modification Strategy | Dimensions | *In-vivo/In-vitro* studies | Bioactivity Evaluation/Conclusion | Ref. |
|---|---|---|---|---|---|---|
| 1 | YSZ with AISI 316-L | Pulsed Electron Deposition | – | – | Working gas pressure strongly affected the surface properties of YSZ films. | [159] |
| 2 | YSZ with silica coatings | Soft lithography and sol-gel | – | Human osteoblast-like cells *in vitro* | Biocompatibility, early alignment of osteoblast-like cells | [160] |
| 3 | YSZ with HA coating on Zirconia discs | Wet powder spraying (WPS) | – | SBF, human osteoblast cells (HOB) *in vitro* | Good mechanical strength, excellent interfacial bonding and bioactivity | [145] |
| 4 | YSZ with reinforced $TiO_2$ | Plasma spray technique | – | SBF *in vitro* | Excellent mechanical stability, highly effective in generating apatite | [161] |
| 6 | HA | Sol-gel, dip coating + calcination | Particle size: ~30 nm | SBF Ringer's solution, *In vitro* Osteoblasts from calvaria of neonatal (<2 days old) Sprague–Dawley rats | Enhanced corrosion resistance | [162] |
| 7 | YSZ with 3% of yttria coating with $Si_3N_4$ particles | Laser cladding | – | SaOS-2 human osteosarcoma cell line *in vitro* | Improved cellular adhesion and bone tissue formation, with higher degrees of maturity and overall better quality | [163] |

HA, hydroxyapatite.

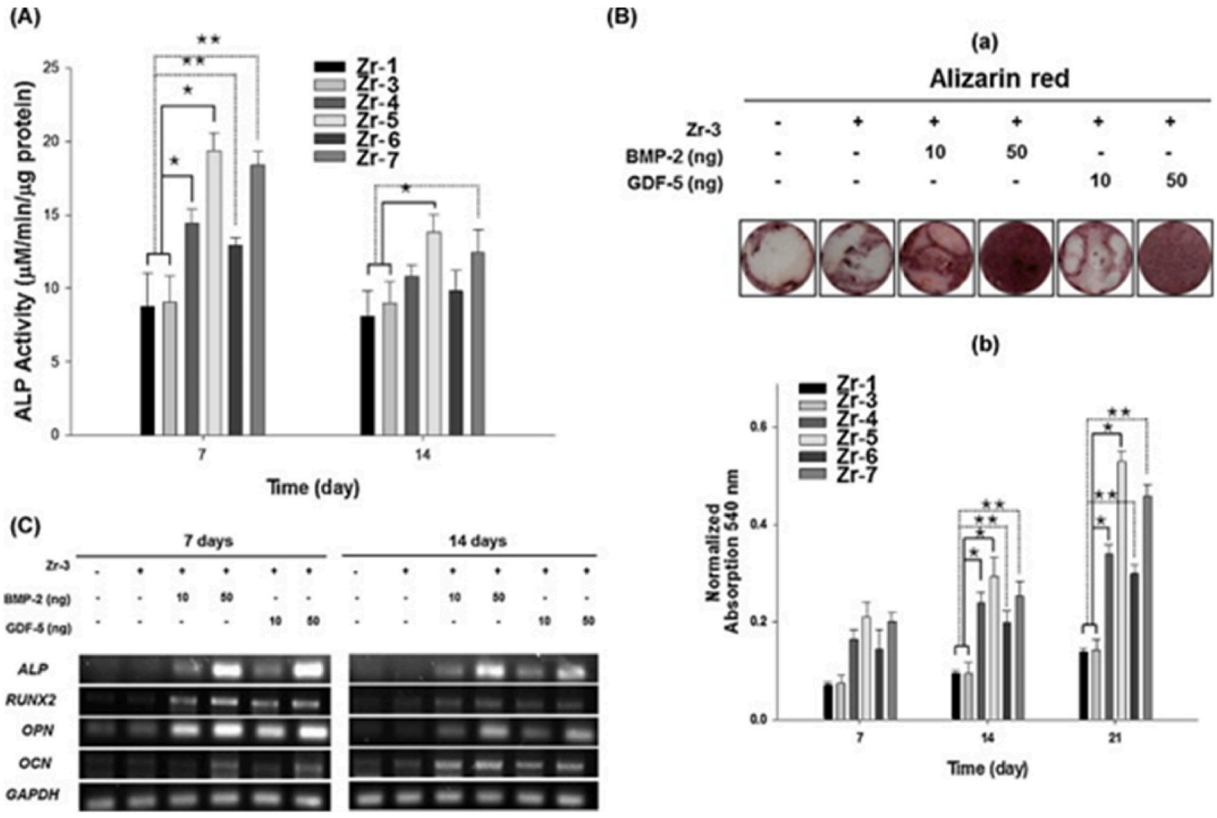


**Fig. 3.** Protein incorporated zirconia implants. Zr-1/Zr-3: Non-coated Zr surface; Zr-4/Zr-5: Bone morphogenetic protein-2 (BMP-2) coated Zr; Zr-6/Zr-7: Growth differentiation factor-5 (GDF-5) coated Zr surface. (A) BMP-2 and GDF-5 coatings augmented *in vitro* alkaline phosphatase (ALP) activity levels of MG-63 osteoblasts at day 7 and 14 on Zr surface. (B) Alizarin red staining showing enhanced calcium deposition from MG-63 osteoblasts on BMP-2 and GDF-5 coated Zr surfaces. (C) Increased mRNA expression of ALP and osteopontin (OPN) from MG-63 cells on BMP-2 and GDF-5 coated Zr surface. Adapted with permission from Ref. [4].

surface treatment. This observation is in contrast to the earlier reported by Att et al. [1]. The efficacy of UV treated Zr cylindrical implants in an *in vivo* rat femoral model was investigated [173] and showed extensive bone formation around UV treated implants after two weeks of implantation, compared to untreated implants. Additionally, enhanced osteogenesis, increased peri-implant bone formation, and better implant-bone integration in the absence of fibrous tissue between the implant surface and the bone was observed after four weeks of implantation.

## 3. Alloyed Zr implants

Conventionally, Zr is alloyed with Ti for improving the mechanical properties of Ti. However, in recent years Zr based alloys have gained importance in implant development attributed to their ability to form an intrinsic bone-like apatite layer on their surfaces upon implantation [174,175]. In certain situations like implantation in a narrow edentulous alveolar bone ridge or the replacement of a single tooth in a narrow gap, small diameter implants of enhanced mechanical/tensile strength are required, and in these cases, the mechanical strength of pure metals like Ti and Zr are insufficient [176,177]. The use of Zr-based alloys, such as TiZr, addresses this problem as they have higher mechanical strength making them ideal candidates for conditions requiring enhanced mechanical properties [177].

### 3.1. Titanium zirconium (TiZr) alloys

The enhanced mechanical properties of TiZr alloy, compared to Ti and Zr alone, make them a suitable candidate for small diameter dental/medical implants, especially in high loading settings. Chen et al. evaluated the effect of alkali heat treatment (AH) followed by soaking in stimulated body fluid (SBF) to coat calcium phosphate on the TiZr surface (AH-SBF) [178]. Samples were initially immersed in 10 M NaOH, then heated to 600 °C for 1 h, then finally immersed in SBF at 37 °C for 30 days. It is important to note that the alloy readily forms metal oxide passive film on the surface, providing corrosion resistance. However, upon alkali treatment, a porous sodium titanate and zirconate hydrogel is formed on the surface of the alloy with a porosity of ~500 nm. Upon immersion in SBF, small cubic particles of CaP deposit on the surface of the material and gradually form a uniform layer of CaP on the porous surface. This apatite mimicking CaP can be used to augment integration with the surrounding bone upon implantation. Elucidation of the oxide layer formed on the surface and the role of Ti and Zr in the formation of sodium titanate and zirconate hydrogel leading to CaP deposition can be obtained via in-depth surface chemistry analysis. Further investigations on the mechanical stability of CaP coatings are also needed.

In 2011, Chen et al. further evaluated the *in vitro* response of human osteoblast-like cells (SaOS2) towards the AH-SBF modified TiZr surfaces [132]. Enhanced cellular alignment with multiple extended filopodial extensions was observed on the modified surfaces. These results provided evidence that modified TiZr surfaces can be used to orchestrate osteogenesis at the bone-implant interface. Subsequently, Grigorescu et al. fabricated nanotubes on the surface of TiZr alloy using a 2-step anodization process using ethylene glycol electrolyte with 15 vol% $H_2O$ and 0.2 M $NH_4F$ [179]. The first step of anodization was carried out for 2 h, followed by removing the formed oxide layer by sonication in de-ionized water, with the second step of anodization carried out for 1 h in the same electrolyte. The anodization at voltages 15 V, 30 V and 45 V, yielded nanotubes of diameter 30–40 nm, 50–60 nm and 80–100 nm, respectively, after the first anodization, which then reduced to 20–30 nm for 15 V, 35–40 nm for 30 V, and 40–70 nm for 45 V upon second anodization. An increase in surface hydrophilicity was observed with

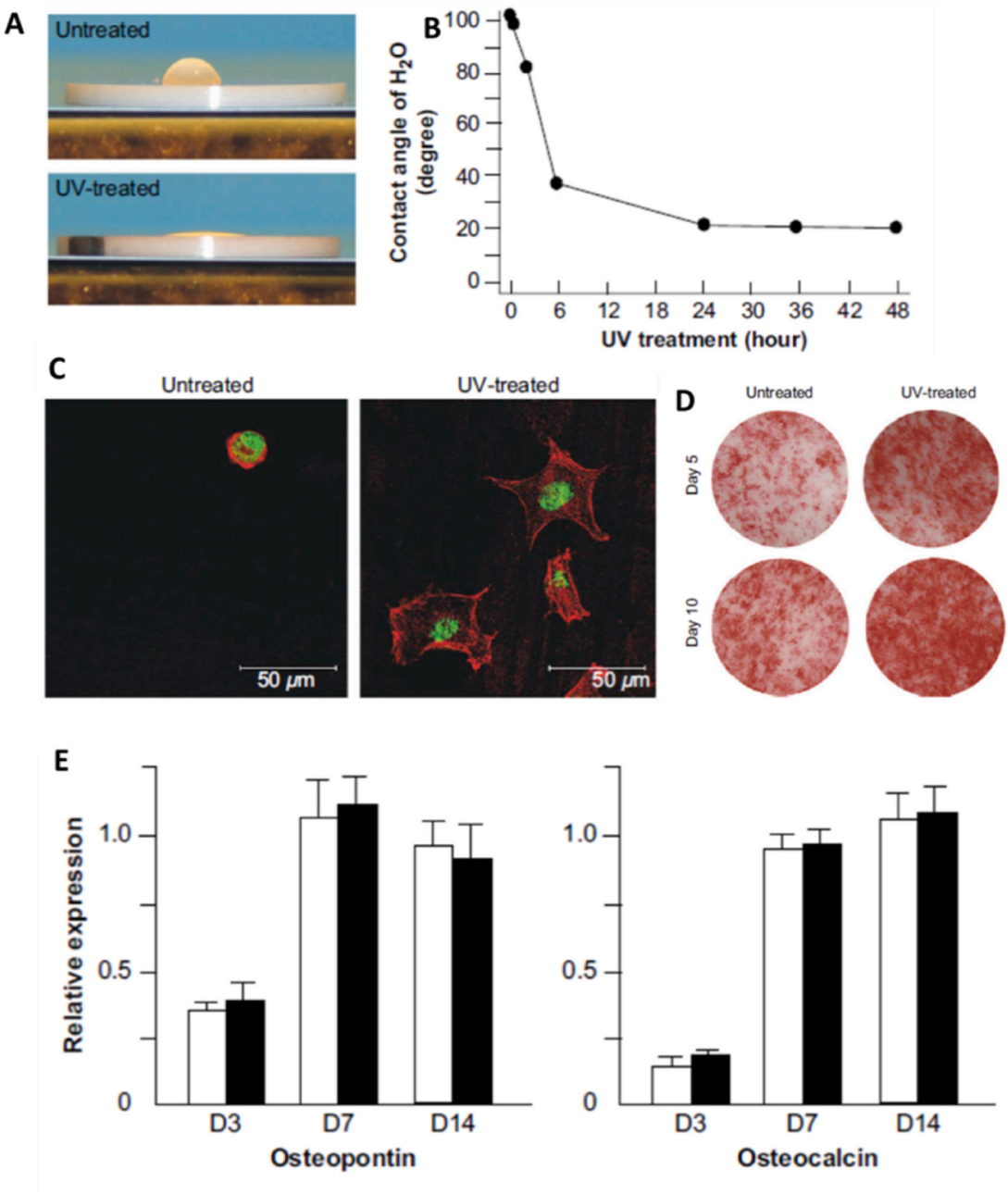


**Fig. 4.** Ultraviolet (UV) irradiated $ZrO_2$ surfaces. (A) Photograph of water droplet on untreated and UV treated $ZrO_2$ surface indicating a shift from hydrophobic to hydrophilic upon UV exposure. (B) Water contact angle of $ZrO_2$ surface at various treatment times. (C) Initial spread and cytoskeleton of osteoblasts (3 h post cell seeding on treated and untreated surface). (D) ALP activity. (E) Osteogenic marker gene expression. Adapted with permission from Ref. [1].

decreasing nanotube diameters.

It is noteworthy that hydrophilic surfaces demonstrate enhanced bacterial anti-adhesive properties [180]. Further, it is established that nanotubular structures, owing to their high surface area and enhanced protein adhesion, augment osteogenesis [181,182]. However, further assessment of antibacterial efficacy and biofilm formation using a polymicrobial system may provide further insight into how these techniques can be applied clinically.

Charles et al. evaluated surface modification of TiZr alloy using neodymium-doped yttrium aluminium garnet (Nd-YAG) laser [183]. Nd-YAG laser at a wavelength of 1064 nm was moved over samples in a linear motion with 8 W power, 300 mJ/pulse energy, and 50-kHz pulse frequency. The roughness of the TiZr surface shifted from 0.03 μm to 0.06 μm upon laser treatment, indicating that lasers roughened the alloy surface. Contact angle analysis confirmed that the laser-treated surface was hydrophilic compared to the untreated surface. Further, surface modification enhanced the adhesion of human osteoblasts *in vitro*. Of particular interest is that the lower roughness of the unmodified surface led to the reduced cellular attachment that further hindered cell-cell interaction. In the laser modified surfaces, focal adhesion areas with dendritic projections and filapodial extensions were observed. Increased mineralization was also observed on the modified surface, indicating the osseointegration potential of laser-treated TiZr surfaces.

Plasma electrolytic oxidation (PEO) has been utilized to form a thick porous coating on Ti surfaces to enhance osteogenesis [184]. The same strategy was employed by Cordeiro et al. to modify the surface of a TiZr alloy and evaluate its effect on protein adsorption and bacterial adhesion [185]. Samples were oxidized in an electrolyte containing calcium

acetate and glycerophosphate disodium at 290 V and 250 Hz. The PEO-treated surface exhibited a porous morphology with higher surface roughness and hydrophilicity than untreated surfaces and subsequently demonstrated a two-fold increase in protein adsorption. Further, a reduction in the number of colony-forming units of *Streptococcus sanguinis* indicated that PEO modification limits bacterial adhesion on TiZr surfaces. Additionally, PEO treatment has been reported to facilitate the incorporation of Ca and P present in the electrolyte onto the porous surface in an atomic ratio comparable to hydroxyapatite [184]. Coatings that mimic natural bone structure have great potential to augment implant-bone integration.

### 3.2. Zirconium Niobium (Zr–1Nb) alloy

Zr–1Nb alloys have higher corrosion and mechanical resistance than Zr, making them suitable candidates for bone and dental implants. Kim et al. evaluated the effect of polishing with abrasive paper (#100, #600, #2400) followed by NaOH treatment of Zr–1Nb alloy surfaces [186]. In addition, the treated surfaces were immersed in simulated body fluid (SBF) to evaluate the rate of surface apatite deposition. It is important to note that the effect of surface morphology on apatite deposition is critical in understanding the *in vivo* bio-mineralization of the implant. An increase in apatite deposition was observed with an increase in surface roughness, with substrates polished using #100 abrasive paper showing higher deposition than #2400 paper polished substrates. Other studies have shown that NaOH-treated Ti–6Al–4V surfaces enhance apatite formation [187]. When Kim et al. compared the effect of NaOH treatment on polished Zr–1Nb surfaces, they did not observe any change in apatite deposition. Therefore, it was concluded that the $ZrO_2$ layer on the alloy surface aids better nucleation of apatite crystals than the $TiO_2$ layer on Ti implants. Consequently, even without NaOH treatment, Zr alloy surfaces have significant potential for bio-mineralization.

## 4. Commercial Zr/$ZrO_2$ implants

Three types of Zr/$ZrO_2$ substrates are commonly utilized to fabricate commercial implant/abutment: yttria-stabilized $ZrO_2$ (Y-TZP), alumina-toughened $ZrO_2$ (ATZ), and hot isostatic pressed (HIP) $ZrO_2$ (Table 6) [188]. Y-TZP is fabricated via sintering the composite of $ZrO_2$ containing 3 mol% yttria, under 1300–1500 °C to yield a tetragonal crystallized Y-TZP. Y-TZP is favoured for its outstanding resistance against corrosion and low thermal degradation (LTD, or $ZrO_2$ ageing), and thus utilized by commercial implant companies including Straumann®, Camlog®, Nobel® and ICX® [189,190]. Fabrication of ATZ involves combining 20 wt% $Al_2O_3$ with 80 wt% TZ-3Y composite ($ZrO_2$ with 3%$Y_2O_3$), pressured in 50 MPa and sintered at 1400 °C for 2 h [191]. ATZ is also corrosion-resistant, with slightly enhanced bioactivity than pure Ti, and is used by Swiss Dental Solutions® (SDS), Nobel® and Zircon Vision® [98]. HIP involves sintering that compresses and densify $ZrO_2$ without altering its chemical compositions, starting at 300 °C and 110 MPa, and continuously increasing to 1200 °C and 205 MPa for 2 h [168,189]. Previous studies have confirmed suitable chemical stability and mechanical strength of HIP-treated $ZrO_2$, used by various implant manufacturers, including Bredent® and Z-systems® [168,189].

**Table 6**
Summary of commercially utilized zirconia implant types.

| | Y-TZP | ATZ | HIP |
|---|---|---|---|
| **Full form** | Yttria-stabilized $ZrO_2$ | Alumina-toughened $ZrO_2$ | Hot isostatic pressed $ZrO_2$ |
| **Fabrication** | Sintering $ZrO_2$ composite containing 3 mol% yttria under 1300–1500 °C | 20 wt% $Al_2O_3$ + 80 wt% TZ-3Y composite, sintered in 50 MPa, 1400 °C for 2 h | Sintering $ZrO_2$ at 1200 °C, 205 MPa for 2 h |
| **Characteristics** | Distinguished corrosion resistance and anti-ageing property | Corrosion-resistant | Pure $ZrO_2$ without chemical changes. Chemically and mechanically stable |
| **Used by Companies** | Straumann®, Camlog®, and ICX® | Swiss Dental Solutions® (SDS), Nobel® and Zircon Vision® | Bredent® and Z-systems® |
| **Crystal phase** | $ZrO_2$ Tetragonal | $Al_2O_3$ Rhombohedral + $ZrO_2$ Tetragonal | $ZrO_2$ Tetragonal |
| **References** | [189,190,192] | [98,191] | [168,189] |

Various surface modifications have been performed on commercial $ZrO_2$ implants to augment tissue integration, as summarized in Table 7 [149,151,153,155,189]. As reported by Kohal et al., the air-borne particle abrasion method effectively enables micro-roughened topographies on the $ZrO_2$ substrate, which are favourable for osseointegration [193]. Hence, sandblasting and acid etching (SLA), commonly applied to fabricate Ti implants, has also been utilized on Zr/$ZrO_2$ implants fabrication (e.g. ZLA® surfaces by Straumann®) [194]. However, it is also reported that the airborne particles abrasion during SLA treatment could alter the crystalline phase of $ZrO_2$ substrates and compromise resistance against low thermal degradation (LTD), undermining long-term stability [189,193]. Besides sandblasting, other techniques to create micro-roughness to augment osseointegration abilities include milling, sintering and ceramic injection moulding (CIM) [189]. Incorporating bioactive coatings (e.g. hydroxyapatite, dopamine) have also been utilized to modify $ZrO_2$ implants [149,151,153,155]. However, limited studies have investigated the long-term surface stability and *in vitro/in vivo* biosafety, which represents a significant research gap towards the clinical translation of such bioactive $ZrO_2$ implants.

To date, various studies have established the clinical reliability of commercial $ZrO_2$ implants, including favourable implant survival rate (ISR) and restricted marginal bone loss (MBL) [195–198]. As Pieralli et al. reported in 2014, among 12 clinical studies published between 2010 and 2015, the overall one-year ISR of commercial $ZrO_2$ implants was 96%, with an average MBL of 0.79 mm after one year [195]. Similarly, Roehling et al. identified 11 clinical studies on commercial $ZrO_2$ implants and showed an average one-year ISR of 94.64% with an MBL of 0.78 mm [196]. These findings are comparable to conventional Ti Implants. Besides predictable osseointegration, the long-term aesthetic outcomes around white-coloured $ZrO_2$ implants/abutments were also favourable [198]. As Naveau et al. reported, peri-implant mucosa discolouration and gingival recession were alleviated around $ZrO_2$ implants compared with the greyish-coloured Ti counterparts, supporting the notion of the superior long-term aesthetics of $ZrO_2$ implant restorations [198]. Such favourable outcomes are attributed to the tooth-like appearance and the chemical stability of $ZrO_2$ implant surfaces [193,199].

## 5. Challenges to clinical translation of zirconia implants

### 5.1. Wear and corrosion

Dental implants are subjected to continuous force during both the implant surgery and the masticatory process throughout the lifetime of the implant [205,206]. These forces can severely affect the stability of the implant surface and its modification, and can result in delamination and ion/particle leaching [168,206]. In addition to general wear and potential fretting corrosions developed during long-term functioning, these issues highlight the need to investigate and further understand the stability of $ZrO_2$ implants to ensure their longevity and biosafety [168].

Compared with other implant materials, $ZrO_2$ has reliable physical and electrochemical stability geared toward the favourable long-term performance of dental implants under the constant physical and chemical corrosive environment within the oral cavity [207]. To this end,

**Table 7**
Surface characteristics and modification strategies of clinically used zirconia implants.

| Company | Implant Name | Material | Modification | Characteristics | Ref |
|---|---|---|---|---|---|
| Straumann® | PURE ceramic® | Y-TZP | $ZrO_2$ sandblast & acid etch (ZLA) | Macroscale and microscale roughened surface | [190] |
| Bredent® | WhiteSKY® | HIP $ZrO_2$ | Sandblasting | One-piece implants only, microscale roughened surface | [200] |
| Camlog® | CERALOG® | Y-TZP | CIM (Ceramic Injection Moulding) | Microscale roughened surface | [201] |
| Nobel® | NobelPearl®/ ZiUnite® | ATZ | Sandblast, acid etch & hydrophilic treatment | Lower plaque accumulation and enhanced soft-tissue integration | [202] |
| Z-systems® | Z5c/Z5m/Z5s® | HIP $ZrO_2$ | Sandblast and laser treatment | Predictable osseointegration | [203] |
| Swiss Dental Solutions® | SDS 1.0/1.1/2.2® | ATZ | Microporous surface by sandblasting | Microroughened surface | – |
| Zircon Vision® | ZV3 series® | ATZ | Milling & sintering | High surface roughness; osseointegration | [204] |
| ICX® | ICX-Active-White® | Y-TZP | N/A | Microroughened surface | – |

Tsumita et al. have reported that the $ZrO_2$ abutment-implant interface can bear repeated loads without any delamination, with a capacity against fatigue for $ZrO_2$ abutments similar to Ti counterparts [207]. Corne et al. compared the stability of Ti, Ti alloy, Y-TZP $ZrO_2$, and Y-TZP coated Ti alloys after 16 h of fretting corrosion in simulated human gingiva, under constant contact pressure (100 MPa) [208]. The results showed enhanced anti-fretting capacity from Y-TZP substrate compared to other groups, and a coating of Y-TZP layer on the Ti surface could also significantly enhance its anti-fretting capacity [208]. It is worth noting that $ZrO_2$ is also widely coated onto other biomedical materials to reduce their electrochemical corrosion[119,209,210].

$ZrO_2$ is known to exist in three prominent crystalline phases: monoclinic, tetragonal, and cubic [205,211]. Tetragonal is the main phase of commercial $ZrO_2$ implants formed under a hydrothermal sintering process with reliable mechanical strength, but exhibits reduced stability compared to the monoclinic phase at room temperature. Thus the tetragonal structure of the $ZrO_2$ implant is slowly transformed into a monoclinic phase at room temperature, known as low-temperature degradation (LTD) [212]. LTD can be accelerated with water/moisture that creates cracks on the $ZrO_2$ surface and compromises its mechanical strength [213]. As such, LTD is a significant challenge towards the long-term stability of $ZrO_2$ implants. Various studies have tried to inhibit the monoclinic transformation of $ZrO_2$ implants and maintain their tetragonal phase [212,214]. One option to stabilize the tetragonal phase $ZrO_2$ is to apply yttria to form the Y-TZP composite, that significantly enhances the physical stability in a humid atmosphere [214]. Zhang et al. reported that adding 3–5% yttria to $ZrO_2$ substrate effectively inhibits monoclinic phase translation and stabilizes the $ZrO_2$ composite against water-induced corrosion [215]. Besides Y-TZP, an alternate strategy to resist water-induced ageing is incorporating Al into the $ZrO_2$ substrate to fabricate an ATZ composite [216]. Spies et al. reported that ATZ composites could bear multiple dynamic loading and hydrothermal/water treatment cycles without crack formation or delamination [216]. Furthermore, tolerating multiple loadings under hydrothermal/humid circumstances, most of the ATZ component remained in the corrosion-resistant tetragonal phase, indicating its reliability for long-term functioning within the oral cavity [216].

### 5.2. Cytotoxicity concerns

Despite the widespread use of Zr-based alloys as orthopaedic/dental implants, mechanical wear and tear can lead to the leaching of $ZrO_2$ nanoparticles (NPs) into the surrounding tissue. Accumulation of NPs can lead to cytotoxicity and even acute organ failure [217]. Ye et al. investigated the effect of $ZrO_2$ NPs on the cellular properties of mouse osteoblast cells *in vitro* [217]. Low concentrations of $ZrO_2$ NPs (0–80 μg/mL) were non-toxic, however, at higher concentrations (100–150 μg/mL) $ZrO_2$ NPs reduced cell viability by 50%. Exposure to the higher concentration of NPs over time led to changes in cellular morphology, an increase in the number of apoptotic and necrotic cells, elevated reactive oxygen species (ROS) levels, and reduced mineralization and osteogenic marker expression, indicating a cytotoxicity effect caused by prolonged exposure and bioaccumulation of $ZrO_2$ NPs.

In another study, He et al. evaluated the potential toxicity effects of Zr implants in mini pig maxillae *in vivo* [109]. Briefly, threaded Ti and $ZrO_2$ implants were inserted in the maxilla's edentulous parts, and no dental superstructure or loading was performed on the implants. The levels of Ti and Zr ions present within the tissues after 12 weeks of implantation were determined by inductively coupled plasma optical emission spectrometry (ICP-OES) and inductively coupled plasma mass spectrometry (ICP-MS). The findings revealed 1.67 ± 0.42 mg/kg-bone weight of Ti and 0.59 ± 0.13 mg/kg-bone weight of Zr in bone slices adjacent to the Ti and $ZrO_2$ implants, respectively. This confirmed that the amount of Zr leaching from implants was low in comparison to their Ti counterparts.

Further, the spatial distribution of isotopes near the implants showed a higher intensity of 47Ti and 90Zr isotopes close to the screw thread tip, indicating that the chances of wear and ion release may be higher in areas of stress. Histological analysis of bone marrow also revealed Ti particles and traces of bone marrow fibrosis in tissues near the Ti implants, which was congruent with previous reports for Ti implants [218]. In contrast, no Zr particles were found in the bone marrow. However, minor bone marrow fibrosis was observed. Overall, the study showed that the leaching of ions and particles are lower in $ZrO_2$ implants. Importantly, these studies were carried out in a mechanically unloaded condition, i.e., not subjected to masticatory forces. Hence, studies incorporating mechanical loading and more accurately resembling physiological conditions would be of value. The authors also compared the cytotoxicity of $ZrO_2$ NPs and $ZrO_2$ microparticles (MPs) in human periodontal ligament cells *in vitro*. EC50 of $ZrO_2$-NPs and $ZrO_2$-MPs was found to be 13.96 mg/mL and 80.99 mg/mL, respectively, indicating that NPs were more toxic than MPs. However, the *in vivo* studies showed that the Zr content near the implant was only 0.75 mg/kg bone, which is 18,613 times lower than the EC50 of $ZrO_2$-NPs, implying that the cytotoxic effect of $ZrO_2$ implants is low. Nevertheless, evaluation of Zr implants and their long term cytocompatibility requires further investigation.

## 6. Conclusions

While titanium may be the popular material choice for dental implants, zirconia based dental implants and abutments are receiving increased attention, which can be attributed to their unique characteristics, including white colour (improved esthetics), reduced bacterial affinity, high flexural strength and high fracture toughness, while maintaining the same osseointegration capacity as titanium. Zirconium and zirconia-based implants hold great promise as contemporary dental implants. In order to achieve enhanced bioactivity and therapeutic potential, various physical, chemical, electrochemical and biological enhancements have been performed, which demonstrate favourable outcomes *in vitro* and *in vivo*. Further, CaP, hydroxyapatite, polydopamine and other biomolecular coatings have enabled enhanced osteogenesis on zirconia implants. Also discussed in this review are the modified alloyed and clinically used Zr implants towards achieving

favourable bioactivity performances. An ideal zirconia implant surface modification would preserve the micro-roughness that to date remains a clinically preferred 'gold standard', while superimposing nano-topography to further enhance bioactivity and enable ease of further biomolecule or therapeutic modification. Despite the progress made, significant research gaps remain, including mechanical stability and local cytotoxicity concerns. The next generation of zirconia implants will be nano-engineered with controlled bioactivity to accelerate implant integration, even in compromised patient conditions.

## Declaration of competing interest

The authors declare that they have no known competing financial interests or personal relationships that could have appeared to influence the work reported in this paper.

## CRediT authorship contribution statement

**Divya Chopra:** Conceptualization, Investigation, Methodology, Formal analysis, Writing – original draft, Visualization. **Anjana Jayasree:** Conceptualization, Writing – review & editing. **Tianqi Guo:** Conceptualization, Writing – review & editing. **Karan Gulati:** Conceptualization, Methodology, Writing – review & editing. **Sašo Ivanovski:** Validation, Writing – review & editing, Supervision, Project administration.

## Acknowledgements

Divya Chopra, Anjana Jayasree and Tianqi Guo are supported by the UQ Graduate School Scholarship (UQGSS) funded by the University of Queensland. Karan Gulati is supported by National Health and Medical Research Council (NHMRC) Early Career Fellowship (APP1140699).

## References

[1] W. Att, M. Takeuchi, T. Suzuki, K. Kubo, M. Anpo, T. Ogawa, Enhanced osteoblast function on ultraviolet light-treated zirconia, Biomaterials 30 (7) (2009) 1273–1280.
[2] K. Regish, D. Sharma, D. Prithviraj, An overview of immediate root analogue zirconia implants, J. Oral Implantol. 39 (2) (2013) 225–233.
[3] F. Carinci, F. Pezzetti, S. Volinia, F. Francioso, D. Arcelli, E. Farina, A. Piattelli, Zirconium oxide: analysis of MG63 osteoblast-like cell response by means of a microarray technology, Biomaterials 25 (2) (2004) 215–228.
[4] M.S. Bae, J.E. Kim, J.B. Lee, D.N. Heo, D.H. Yang, J.-H. Kim, K.-R. Kwon, J. B. Bang, H. Bae, I.K. Kwon, ZrO2 surface chemically coated with hyaluronic acid hydrogel loading GDF-5 for osteogenesis in dentistry, Carbohydr. Polym. 92 (1) (2013) 167–175.
[5] L.C. Trincă, D. Mareci, R.M. Souto, A.D. Lozano-Gorrín, J. Izquierdo, L. Burtan, I. Motrescu, V. Vulpe, G. Pavel, S. Strungaru, I. Stoleriu, A.L. Strat, C. Solcan, Osseointegration evaluation of ZrTi alloys with hydroxyapatite-zirconia-silver layer in pig's tibiae, Appl. Surf. Sci. 487 (2019) 127–137.
[6] J. Chevalier, What future for zirconia as a biomaterial? Biomaterials 27 (4) (2006) 535–543.
[7] N. Cionca, D. Hashim, A. Mombelli, Zirconia dental implants: where are we now, and where are we heading? Periodontol. 2000 73 (1) (2017) 241–258.
[8] R. van Brakel, H.J. Noordmans, J. Frenken, R. de Roode, G.C. de Wit, M.S. Cune, The effect of zirconia and titanium implant abutments on light reflection of the supporting soft tissues, Clin. Oral Implants Res. 22 (10) (2011) 1172–1178.
[9] K. Muller, E. Valentine-Thon, Hypersensitivity to titanium: clinical and laboratory evidence, Neuroendocrinol. Lett. 27 (1) (2006) 31–35.
[10] D. Weingart, S. Steinemann, W. Schilli, J. Strub, U. Hellerich, J. Assenmacher, J. Simpson, Titanium deposition in regional lymph nodes after insertion of titanium screw implants in maxillofacial region, Int. J. Oral Maxillofac. Surg. 23 (6) (1994) 450–452.
[11] F. Toumelin-Chemla, F. Rouelle, G. Burdairon, Corrosive properties of fluoride-containing odontologic gels against titanium, J. Dent. 24 (1–2) (1996) 109–115.
[12] S. Sridhar, T.G. Wilson Jr., K.L. Palmer, P. Valderrama, M.T. Mathew, S. Prasad, M. Jacobs, I.M. Gindri, D.C. Rodrigues, In vitro investigation of the effect of oral bacteria in the surface oxidation of dental implants, Clin. Implant Dent. Relat. Res. 17 (2015) e562–e575.
[13] J.R. Kelly, I. Denry, Stabilized zirconia as a structural ceramic: an overview, Dent. Mater. 24 (3) (2008) 289–298.
[14] S.F. Janner, M. Gahlert, D.D. Bosshardt, S. Roehling, S. Milz, F. Higginbottom, D. Buser, D.L. Cochran, Bone response to functionally loaded, two-piece zirconia implants: a preclinical histometric study, Clin. Oral Implants Res. 29 (3) (2018) 277–289.
[15] S. Roehling, M. Astasov-Frauenhoffer, I. Hauser-Gerspach, O. Braissant, H. Woelfler, T. Waltimo, H. Kniha, M. Gahlert, In vitro biofilm formation on titanium and zirconia implant surfaces, J. Periodontol. 88 (3) (2017) 298–307.
[16] N. Nomura, K. Oya, Y. Tanaka, R. Kondo, H. Doi, Y. Tsutsumi, T. Hanawa, Microstructure and magnetic susceptibility of as-cast Zr-Mo alloys, Acta Biomater. 6 (3) (2010) 1033–1038.
[17] R. Kondo, Y. Tsutsumi, H. Doi, N. Nomura, T. Hanawa, Effects of phase constitution on magnetic susceptibility and mechanical properties of Zr-rich Zr-Mo alloys, Acta Biomater. 7 (12) (2011) 4259–4266.
[18] L. Saldaña, A. Mendez-Vilas, L. Jiang, M. Multigner, J.L. González-Carrasco, M. T. Pérez-Prado, M.L. Gonzalez-Martin, L. Munuera, N. Vilaboa, In vitro biocompatibility of an ultrafine grained zirconium, Biomaterials 28 (30) (2007) 4343–4354.
[19] Y. Ichikawa, Y. Akagawa, H. Nikai, H. Tsuru, Tissue compatibility and stability of a new zirconia ceramic in vivo, J. Prosthet. Dent 68 (2) (1992) 322–326.
[20] I. Ahmad, Yttrium-partially stabilized zirconium dioxide posts: an approach to restoring coronally compromised nonvital teeth, Int. J. Periodontics Restor. Dent. 18 (5) (1998) 454–465.
[21] T. Guo, K. Gulati, H. Arora, P. Han, B. Fournier, S. Ivanovski, Orchestrating Soft Tissue Integration at the Transmucosal Region of Titanium Implants, Acta Biomater 124 (2021) 33–49.
[22] K. Gulati, S. Ivanovski, Dental implants modified with drug releasing titania nanotubes: therapeutic potential and developmental challenges, Expert Opin. Drug Deliv. 14 (8) (2017) 1009–1024.
[23] D. Chopra, K. Gulati, S. Ivanovski, Understanding and optimizing the antibacterial functions of anodized nano-engineered titanium implants, Acta Biomater. 127 (2021) 80–101.
[24] U. Salihoğlu, D. Boynueğri, D. Engin, A.N. Duman, P. Gökalp, K. Baloş, Bacterial adhesion and colonization differences between zirconium oxide and titanium alloys: an in vivo human study, Int. J. Oral Maxillofac. Implants 26 (1) (2011).
[25] C. Do Nascimento, M.S. Pita, E. de Souza Santos, N. Monesi, V. Pedrazzi, R.F. de Albuquerque Junior, R.F. Ribeiro, Microbiome of titanium and zirconia dental implants abutments, Dent. Mater. 32 (1) (2016) 93–101.
[26] K. Gulati, S.M. Hamlet, S. Ivanovski, Tailoring the Immuno-Responsiveness of Anodized Nano-Engineered Titanium Implants, J Mater. Chem. B 6 (2018) 2677–2689.
[27] K. Gulati, M. Kogawa, S. Maher, G. Atkins, D. Findlay, D. Losic, Titania Nanotubes for Local Drug Delivery from Implant Surfaces", in: D. Losic, A. Santos (Eds.), in book Electrochemically Engineered Nanoporous Materials: Methods, Properties and Applications, (Springer International Publishing AG - Germany). Springer Series in Materials Science 220, 2015 https://doi.org/10.1007/978-3-319-20346-1_10. https://link.springer.com/chapter/10.1007%2F978-3-319-20346-1_10.
[28] T. Guo, K. Gulati, H. Arora, P. Han, B. Fournier, S. Ivanovski, Race to Invade: Understanding Soft Tissue Integration at the Transmucosal Region of Titanium Dental Implants, Dent. Mater 37 (2021) 816–831.
[29] F. Rupp, L. Liang, J. Geis-Gerstorfer, L. Scheideler, F. Hüttig, Surface characteristics of dental implants: A review, Dent. Mater. 34 (1) (2018) 40–57.
[30] A.G. Sanchez, W. Schreiner, G. Duffó, S. Ceré, Surface characterization of anodized zirconium for biomedical applications, Appl. Surf. Sci. 257 (15) (2011) 6397–6405.
[31] F.H. Schünemann, M.E. Galárraga-Vinueza, R. Magini, M. Fredel, F. Silva, J.C. M. Souza, Y. Zhang, B. Henriques, Zirconia surface modifications for implant dentistry, Mater. Sci. Eng. C Mater. Biol. Appl. 98 (2019) 1294–1305.
[32] R.J. Kohal, F.S. Schwindling, M. Bächle, B.C. Spies, Peri-implant bone response to retrieved human zirconia oral implants after a 4-year loading period: A histologic and histomorphometric evaluation of 22 cases, J. Biomed. Mater. Res. B Appl. Biomater. 104 (8) (2016) 1622–1631.
[33] A. Jayasree, S. Ivanovski, K. Gulati, ON or OFF: triggered therapies from anodized nano-engineered titanium implants, J. Control Release 333 (2021) 521–535.
[34] C. Sanon, J. Chevalier, T. Douillard, M. Cattani-Lorente, S.S. Scherrer, L. Gremillard, A new testing protocol for zirconia dental implants, Dent. Mater. 31 (1) (2015) 15–25.
[35] I. Gnilitskyi, M. Pogorielov, R. Viter, A.M. Ferraria, A.P. Carapeto, O. Oleshko, L. Orazi, O. Mishchenko, Cell and tissue response to nanotextured Ti6Al4V and Zr implants using high-speed femtosecond laser-induced periodic surface structures, Nanomed. Nanotechnol. Biol. Med. 21 (2019) 102036.
[36] A. Almaguer-Flores, P. Silva-Bermudez, R. Galicia, S.E. Rodil, Bacterial adhesion on amorphous and crystalline metal oxide coatings, Mater. Sci. Eng. C 57 (2015) 88–99.
[37] M.F. Kunrath, M.S. Monteiro, S. Gupta, R. Hubler, S.D. de Oliveira, Influence of titanium and zirconia modified surfaces for rapid healing on adhesion and biofilm formation of Staphylococcus epidermidis, Arch. Oral Biol. 117 (2020) 104824.
[38] M. Sowa, M. Piotrowska, M. Widziołek, G. Dercz, G. Tylko, T. Gorewoda, A. M. Osyczka, W. Simka, Bioactivity of coatings formed on Ti–13Nb–13Zr alloy using plasma electrolytic oxidation, Mater. Sci. Eng. C 49 (2015) 159–173.
[39] H. Bakhsheshi-Rad, E. Hamzah, A. Ismail, M. Aziz, M. Kasiri-Asgarani, E. Akbari, S. Jabbarzare, A. Najafinezhad, Z. Hadisi, Synthesis of a novel nanostructured zinc oxide/baghdadite coating on Mg alloy for biomedical application: in-vitro degradation behavior and antibacterial activities, Ceram. Int. 43 (17) (2017) 14842–14850.
[40] V.K. Balla, W. Xue, S. Bose, A. Bandyopadhyay, Laser-assisted Zr/ZrO2 coating on Ti for load-bearing implants, Acta Biomater. 5 (7) (2009) 2800–2809.
[41] B. Bacchelli, G. Giavaresi, M. Franchi, D. Martini, V. De Pasquale, A. Trirè, M. Fini, R. Giardino, A. Ruggeri, Influence of a zirconia sandblasting treated

surface on peri-implant bone healing: An experimental study in sheep, Acta Biomater. 5 (6) (2009) 2246–2257.
[42] Y. Zhang, B.R. Lawn, K.A. Malament, V.P. Thompson, E.D. Rekow, Damage accumulation and fatigue life of particle-abraded ceramics, Int. J. Prosthodont . 19 (5) (2006) 442–448.
[43] T. Tuna, M. Wein, M. Swain, J. Fischer, W. Att, Influence of ultraviolet photofunctionalization on the surface characteristics of zirconia-based dental implant materials, Dent. Mater. 31 (2) (2015) e14–e24.
[44] L. Hao, J. Lawrence, K.S. Chian, Osteoblast cell adhesion on a laser modified zirconia based bioceramic, J. Mater. Sci. Mater. Med . 16 (8) (2005) 719–726.
[45] R.A. Delgado-Ruiz, M. Abboud, G. Romanos, A. Aguilar-Salvatierra, G. Gomez-Moreno, J.L. Calvo-Guirado, Peri-implant bone organization surrounding zirconia-microgrooved surfaces circularly polarized light and confocal laser scanning microscopy study, Clin. Oral Implants Res . 26 (11) (2015) 1328–1337.
[46] E. Karamian, M.R.K. Motamedi, A. Khandan, P. Soltani, S. Maghsoudi, An in vitro evaluation of novel NHA/zircon plasma coating on 316L stainless steel dental implant, Prog. Nat. Sci.: Mater. Int. 24 (2) (2014) 150–156.
[47] M. Cheng, Y. Qiao, Q. Wang, H. Qin, X. Zhang, X. Liu, Dual ions implantation of zirconium and nitrogen into magnesium alloys for enhanced corrosion resistance, antimicrobial activity and biocompatibility, Colloids Surf. B Biointerfaces 148 (2016) 200–210.
[48] A. Ivanova, M. Surmeneva, V. Shugurov, N. Koval, I. Shulepov, R. Surmenev, Physico-mechanical properties of Ti-Zr coatings fabricated via ion-assisted arc-plasma deposition, Vacuum 149 (2018) 129–133.
[49] M. Sandhyarani, M. Ashfaq, T. Arunnellaiappan, M. Selvan, S. Subramanian, N. Rameshbabu, Effect of electrical parameters on morphology and in-vitro corrosion resistance of plasma electrolytic oxidized films formed on zirconium, Surf. Coating. Technol. 269 (2015) 286–294.
[50] D. Liu, T. Yang, H. Ma, Y. Liang, The microstructure, bio-tribological properties, and biocompatibility of titanium surfaces with graded zirconium incorporation in amorphous carbon bioceramic composite films, Surf. Coating. Technol. 385 (2020) 125391.
[51] W. Yuan, D. Xia, Y. Zheng, X. Liu, S. Wu, B. Li, Y. Han, Z. Jia, D. Zhu, L. Ruan, Controllable biodegradation and enhanced osseointegration of ZrO2-nanofilm coated Zn-Li alloy: in vitro and in vivo studies, Acta Biomater. 105 (2020) 290–303.
[52] K. Gulati, J.-C. Scimeca, S. Ivanovski, E. Verron, Double-edged Sword: Therapeutic Efficacy versus Toxicity Evaluations of Doped Titanium Implants, Drug Discov. Today (2021). https://doi.org/10.1016/j.drudis.2021.07.004.
[53] J. Oliva, X. Oliva, J.D. Oliva, Five-year success rate of 831 consecutively placed zirconia dental implants in humans: a comparison of three different rough surfaces, Int. J. Oral Maxillofac. Implants 25 (2) (2010) 336–344.
[54] R. Depprich, H. Zipprich, M. Ommerborn, C. Naujoks, H.-P. Wiesmann, S. Kiattavorncharoen, H.-C. Lauer, U. Meyer, N.R. Kübler, J. Handschel, Osseointegration of zirconia implants compared with titanium: an in vivo study, Head Face Med . 4 (2008) 1–8.
[55] M. Morra, C. Cassinelli, G. Bruzzone, A. Carpi, G.D. Santi, R. Giardino, M. Fini, Surface chemistry effects of topographic modification of titanium dental implant surfaces: 1. Surface analysis, Int. J. Oral Maxillofac. Implants 18 (1) (2003).
[56] U. Meyer, A. Buchter, H. Wiesmann, U. Joos, D. Jones, Basic reactions of osteoblasts on structured material surfaces, Eur. Cell. Mater. 9 (2005) 39–49.
[57] S. Roehling, M. Astasov-Frauenhoffer, I. Hauser-Gerspach, O. Braissant, H. Woelfler, T. Waltimo, H. Kniha, M. Gahlert, In vitro biofilm formation on titanium and zirconia implant surfaces, J. Periodontol . 88 (3) (2017) 298–307.
[58] H. Xie, S. Shen, M. Qian, F. Zhang, C. Chen, F.R. Tay, Effects of acid treatment on dental zirconia: an in vitro study, PLoS One 10 (8) (2015), e0136263.
[59] G.-J. Oh, J.-H. Yoon, V.T. Vu, M.-K. Ji, J.-H. Kim, J.-W. Kim, E.-K. Yim, J.-C. Bae, C. Park, et al., Surface Characteristics of Bioactive Glass-Infiltrated Zirconia with Different Hydrofluoric Acid Etching Conditions, J. Nanosci. Nanotechnol. 17 (4) (2017) 2645–2648.
[60] U. Hempel, T. Hefti, M. Kalbacova, C. Wolf-Brandstetter, P. Dieter, F. Schlottig, Response of osteoblast-like SAOS-2 cells to zirconia ceramics with different surface topographies, Clin. Oral Impl. Res. 21 (2) (2010) 174–181.
[61] A. Liñares, L. Grize, F. Muñoz, B.E. Pippenger, M. Dard, O. Domken, J. Blanco-Carrión, Histological assessment of hard and soft tissues surrounding a novel ceramic implant: a pilot study in the minipig, J. Clin. Periodontol . 43 (6) (2016) 538–546.
[62] U. Hempel, T. Hefti, M. Kalbacova, C. Wolf-Brandstetter, P. Dieter, F. Schlottig, Response of osteoblast-like SAOS-2 cells to zirconia ceramics with different surface topographies, Clin. Oral Implants Res. 21 (2) (2010) 174–181.
[63] H. Sato, K. Yamada, G. Pezzotti, M. Nawa, S. Ban, Mechanical properties of dental zirconia ceramics changed with sandblasting and heat treatment, Dent. Mater. J . 27 (3) (2008) 408–414.
[64] X. He, F.-X. Reichl, S. Milz, B. Michalke, X. Wu, C.M. Sprecher, Y. Yang, M. Gahlert, S. Röhling, H. Kniha, Titanium and zirconium release from titanium- and zirconia implants in mini pig maxillae and their toxicity in vitro, Dent. Mater. 36 (3) (2020) 402–412.
[65] E. Długoń, K. Pach, M. Gawęda, R. Jadach, A. Wajda, M. Leśniak, A. Benko, M. Dziadek, M. Sowa, W. Simka, Anticorrosive ZrO2 and ZrO2-SiO2 layers on titanium substrates for biomedical applications, Surf. Coating. Technol. 331 (2017) 221–229.
[66] G. Mendonça, D.B.S. Mendonça, L.G.P. Simões, A.L. Araújo, E.R. Leite, A.L. Golin, F.J. Aragão, L.F. Cooper, Nanostructured implant surface effect on osteoblast gene expression and bone-to-implant contact in vivo, Mater. Sci. Eng. C 31 (8) (2011) 1809–1818.
[67] K. Gulati, H.-J. Moon, T. Li, P.S. Kumar, S. Ivanovski, Titania nanopores with dual micro-/nano-topography for selective cellular bioactivity, Mater. Sci. Eng. C 91 (2018) 624–630.
[68] K. Gulati, S. Maher, S. Chandrasekaran, D.M. Findlay, D. Losic, Conversion of titania (TiO 2) into conductive titanium (Ti) nanotube arrays for combined drug-delivery and electrical stimulation therapy, J. Mater. Chem. B 4 (3) (2016) 371–375.
[69] K. Gulati, T. Li, S. Ivanovski, Consume or conserve: microroughness of titanium implants toward fabrication of dual micro-nano topography, ACS Biomater. Sci. Eng. 4 (9) (2018) 3125–3131.
[70] T. Guo, N.A.K. Oztug, P. Han, S. Ivanovski, K. Gulati, Old is gold: electrolyte aging influences the topography, chemistry, and bioactivity of anodized TiO2 nanopores, ACS Appl. Mater. Interfaces 13 (7) (2021) 7897–7912.
[71] S. Rahman, K. Gulati, M. Kogawa, G.J. Atkins, P. Pivonka, D.M. Findlay, D. Losic, Drug diffusion, integration, and stability of nanoengineered drug-releasing implants in bone ex-vivo, J. Biomed. Mater. Res. 104 (3) (2016) 714–725.
[72] L. Wang, Electrochemical behaviour of anodic zirconium oxide nanotubes in simulated body fluid, Appl. Surf. Sci. 258 (2012) 4830–4833.
[73] N. Bashirom, K.A. Razak, C.K. Yew, Z. Lockman, Effect of fluoride or chloride ions on the morphology of ZrO2 thin film grown in ethylene glycol electrolyte by anodization, Procedia Chem. 19 (2016) 611–618.
[74] S. Berger, F. Jakubka, P. Schmuki, Formation of hexagonally ordered nanoporous anodic zirconia, Electrochem. Commun. 10 (2008) 1916–1919.
[75] J. Zhao, R. Xu, X. Wang, Y. Li, In situ synthesis of zirconia nanotube crystallines by direct anodization, Corrosion Sci. 50 (6) (2008) 1593–1597.
[76] S. Ismail, Z.A. Ahmad, A. Berenov, Z. Lockman, Effect of applied voltage and fluoride ion content on the formation of zirconia nanotube arrays by anodic oxidation of zirconium, Corrosion Sci. 53 (4) (2011) 1156–1164.
[77] H. Tsuchiya, J.M. Macak, L. Taveira, P. Schmuki, Fabrication and characterization of smooth high aspect ratio zirconia nanotubes, Chem. Phys. Lett. 410 (4–6) (2005) 188–191.
[78] D. Chopra, K. Gulati, S. Ivanovski, Towards clinical translation: optimized fabrication of controlled nanostructures on implant-relevant curved zirconium surfaces, Nanomaterials 11 (4) (2021) 868.
[79] D. Chopra, K. Gulati, S. Ivanovski, Micro+ nano: conserving the gold standard microroughness to nanoengineer zirconium dental implants, ACS Biomater. Sci. Eng. 7 (7) (2021) 3069–3074.
[80] L.-N. Wang, J.-L. Luo, Electrochemical behaviour of anodic zirconium oxide nanotubes in simulated body fluid, Appl. Surf. Sci. 258 (10) (2012) 4830–4833.
[81] M.R. Katunar, A.G. Sanchez, A.S. Coquillat, A. Civantos, E.M. Campos, J. Ballarre, T. Vico, M. Baca, V. Ramos, S. Cere, In vitro and in vivo characterization of anodised zirconium as a potential material for biomedical applications, Mater. Sci. Eng. C 75 (2017) 957–968.
[82] M.F.T. de la Hoz, M.R. Katunar, A. González, A.G. Sanchez, A.O. Díaz, S. Ceré, Effect of anodized zirconium implants on early osseointegration process in adult rats: a histological and histomorphometric study, Prog. Biomater. 8 (4) (2019) 249–260.
[83] C.J. Frandsen, K.S. Brammer, K. Noh, L.S. Connelly, S. Oh, L.-H. Chen, S. Jin, Zirconium oxide nanotube surface prompts increased osteoblast functionality and mineralization, Mater. Sci. Eng. C 31 (8) (2011) 1716–1722.
[84] L.-N. Wang, C. Shen, A. Shinbine, J.-L. Luo, Variation on wettability of anodic zirconium oxide nanotube surface, Thin Solid Films 531 (2013) 277–283.
[85] D.H. Shin, T. Shokuhfar, C.K. Choi, S.-H. Lee, C. Friedrich, Wettability changes of TiO2 nanotube surfaces, Nanotechnology 22 (31) (2011) 315704.
[86] V. Anitha, J.-H. Lee, J. Lee, A.N. Banerjee, S.W. Joo, B.K. Min, Biofilm formation on a TiO2 nanotube with controlled pore diameter and surface wettability, Nanotechnology 26 (6) (2015), 065102.
[87] T. Li, K. Gulati, N. Wang, Z. Zhang, S. Ivanovski, Bridging the gap: optimized fabrication of robust titania nanostructures on complex implant geometries towards clinical translation, J. Colloid Interface Sci. 529 (2018) 452–463.
[88] K. Gulati, H.-J. Moon, P.S. Kumar, P. Han, S. Ivanovski, Anodized anisotropic titanium surfaces for enhanced guidance of gingival fibroblasts, Mater. Sci. Eng. C 112 (2020) 110860.
[89] M.F. Kunrath, M.S.G. Monteiro, S. Gupta, R. Hubler, S.D. de Oliveira, Influence of titanium and zirconia modified surfaces for rapid healing on adhesion and biofilm formation of Staphylococcus epidermidis, Arch. Oral Biol. 117 (2020) 104824.
[90] B. Bacchelli, G. Giavaresi, M. Franchi, D. Martini, V. De Pasquale, A. Trirè, M. Fini, R. Giardino, A. Ruggeri, Influence of a zirconia sandblasting treated surface on peri-implant bone healing: an experimental study in sheep, Acta Biomater. 5 (6) (2009) 2246–2257.
[91] M. Bosetti, E. Vernè, M. Ferraris, A. Ravaglioli, M. Cannas, In vitro characterisation of zirconia coated by bioactive glass, Biomaterials 22 (9) (2001) 987–994.
[92] V. Koshuro, M. Fomina, A. Voyko, I. Rodionov, A. Zakharevich, A. Skaptsov, A. Fomin, Surface morphology of zirconium after treatment with high-frequency currents, Compos. Struct. 202 (2018) 210–215.
[93] M. Kunrath, M. Monteiro, S. Gupta, R. Hubler, S. de Oliveira, Influence of Titanium and Zirconia modified surfaces for rapid healing on adhesion and biofilm formation of Staphylococcus epidermidis, Arch. Oral Biol. 117 (2020) 104824.
[94] J.M. Cordeiro, B.E. Nagay, A.L.R. Ribeiro, N.C. da Cruz, E.C. Rangel, L.M.G. Fais, L.G. Vaz, V.A.R. Barão, Functionalization of an experimental Ti-Nb-Zr-Ta alloy with a biomimetic coating produced by plasma electrolytic oxidation, J. Alloys Compd. 770 (2019) 1038–1048.

[95] S. Thanka Rajan, A. Bendavid, B. Subramanian, Cytocompatibility assessment of Ti-Nb-Zr-Si thin film metallic glasses with enhanced osteoblast differentiation for biomedical applications, Colloids Surf. B Biointerfaces 173 (2019) 109–120.
[96] M.-T. Tsai, Y.-Y. Chang, H.-L. Huang, Y.-H. Wu, T.-M. Shieh, Micro-arc oxidation treatment enhanced the biological performance of human osteosarcoma cell line and human skin fibroblasts cultured on titanium–zirconium films, Surf. Coating. Technol. 303 (2016) 268–276.
[97] R. Huang, H. Zhuang, Y. Han, Second-phase-dependent grain refinement in Ti–25Nb–3Mo–3Zr–2Sn alloy and its enhanced osteoblast response, Mater. Sci. Eng. C 35 (2014) 144–152.
[98] H.-C. Ko, J.-S. Han, M. Bächle, J.-H. Jang, S.-W. Shin, D.-J. Kim, Initial osteoblast-like cell response to pure titanium and zirconia/alumina ceramics, Dent. Mater. 23 (11) (2007) 1349–1355.
[99] D.-j. Kong, D. Long, Y.-z. Wu, C.-z. Zhou, Mechanical properties of hydroxyapatite-zirconia coatings prepared by magnetron sputtering, Trans. Nonferrous Metals Soc. China 22 (1) (2012) 104–110.
[100] Y.-H. Jeong, H.-C. Choe, W.A. Brantley, I.-B. Sohn, Hydroxyapatite thin film coatings on nanotube-formed Ti–35Nb–10Zr alloys after femtosecond laser texturing, Surf. Coating. Technol. 217 (2013) 13–22.
[101] C. Wang, F. Ma, P. Liu, J. Chen, X. Liu, K. Zhang, W. Li, Q. Han, The influence of alloy elements in Ti6Al4V and Ti35Nb2Ta3Zr on the structure, morphology and properties of MAO coatings, Vacuum 157 (2018) 229–236.
[102] J. Li, X. Zhang, X. He, R. Hang, X. Huang, B. Tang, Preparation, biocompatibility and wear resistance of microstructured Zr and ZrO2 alloyed layers on 316L stainless steel, Mater. Lett. 203 (2017) 24–27.
[103] N. Li, K. Yuan, Y. Song, J. Cao, L. Xu, J. Xu, Plasma Electrolytic Oxidation of Zircaloy-2 Alloy in Potassium Hydroxide/sodium Silicate Electrolytes: the Effect of Silicate Concentration, Boletín de la Sociedad Española de Cerámica y Vidrio, 2020, Boletín de la Sociedad Española de Cerámica y Vidrio 60 (5), 2021 328–336.
[104] J.M. Cordeiro, H.N. Pantaroto, E.M. Paschoaleto, E.C. Rangel, N.C.d. Cruz, C. Sukotjo, V.A.R. Barão, Synthesis of biofunctional coating for a TiZr alloy: surface, electrochemical, and biological characterizations, Appl. Surf. Sci. 452 (2018) 268–278.
[105] A.A. Ivanova, M.A. Surmeneva, V.V. Shugurov, N.N. Koval, I.A. Shulepov, R. A. Surmenev, Physico-mechanical properties of Ti-Zr coatings fabricated via ion-assisted arc-plasma deposition, Vacuum 149 (2018) 129–133.
[106] C. Liu, Y. Zhao, Y. Chen, P. Liu, K. Cai, Surface modification of magnesium alloy via cathodic plasma electrolysis and its influence on corrosion resistance and cytocompatibility, Mater. Lett. 132 (2014) 15–18.
[107] W. Yuan, D. Xia, Y. Zheng, X. Liu, S. Wu, B. Li, Y. Han, Z. Jia, D. Zhu, L. Ruan, K. Takashima, Y. Liu, Y. Zhou, Controllable biodegradation and enhanced osseointegration of ZrO2-nanofilm coated Zn-Li alloy: in vitro and in vivo studies, Acta Biomater. 105 (2020) 290–303.
[108] S. M, A. M, A. T, M.P. S, S. S, R. N, Effect of electrical parameters on morphology and in-vitro corrosion resistance of plasma electrolytic oxidized films formed on zirconium, Surf. Coating. Technol. 269 (2015) 286–294.
[109] X. He, F.-X. Reichl, S. Milz, B. Michalke, X. Wu, C.M. Sprecher, Y. Yang, M. Gahlert, S. Röhling, H. Kniha, R. Hickel, C. Högg, Titanium and zirconium release from titanium- and zirconia implants in mini pig maxillae and their toxicity in vitro, Dent. Mater. 36 (3) (2020) 402–412.
[110] M. Gahlert, S. Roehling, C.M. Sprecher, H. Kniha, S. Milz, K. Bormann, In vivo performance of zirconia and titanium implants: a histomorphometric study in mini pig maxillae, Clin. Oral Implants Res. 23 (3) (2012) 281–286.
[111] M. Rottmar, E. Müller, S. Guimond-Lischer, M. Stephan, S. Berner, K. Maniura-Weber, Assessing the osteogenic potential of zirconia and titanium surfaces with an advanced in vitro model, Dent. Mater. 35 (1) (2019) 74–86.
[112] M. Hirano, Y. Yokoiwa, S. Komai, N. Ohtsu, Enhanced calcification of osteoblast-like cells on zirconium through calcium-phosphate slurry processing, Appl. Surf. Sci. 478 (2019) 567–573.
[113] S. M, P. T, R. N, Role of electrolyte composition on structural, morphological and in-vitro biological properties of plasma electrolytic oxidation films formed on zirconium, Appl. Surf. Sci. 317 (2014) 198–209.
[114] J.M. Cordeiro, L.P. Faverani, C.R. Grandini, E.C. Rangel, N.C. da Cruz, F.H. Nociti Junior, A.B. Almeida, F.B. Vicente, B.R.G. Morais, V.A.R. Barão, W.G. Assunção, Characterization of chemically treated Ti-Zr system alloys for dental implant application, Mater. Sci. Eng. C 92 (2018) 849–861.
[115] M. Murphy, M.S. Walczak, A.G. Thomas, N. Silikas, S. Berner, R. Lindsay, Toward optimizing dental implant performance: surface characterization of Ti and TiZr implant materials, Dent. Mater. 33 (1) (2017) 43–53.
[116] M. Gómez-Florit, R. Xing, J.M. Ramis, S. Taxt-Lamolle, H.J. Haugen, S. P. Lyngstadaas, M. Monjo, Human gingival fibroblasts function is stimulated on machined hydrided titanium zirconium dental implants, J. Dent. 42 (1) (2014) 30–38.
[117] H.I. Arrieta-Oliva, R.I. Gutiérrez-Ventura, D.A. Sánchez-Téllez, L. Téllez-Jurado, B.E. García-Pérez, Osteoblast response to zirconia modified-ORMOSILs, Mater. Sci. Eng. C 109 (2020) 110546.
[118] G. Mendonça, D.B.S. Mendonça, L.G.P. Simões, A.L. Araújo, E.R. Leite, A.L. Golin, F.J.L. Aragão, L.F. Cooper, Nanostructured implant surface effect on osteoblast gene expression and bone-to-implant contact in vivo, Mater. Sci. Eng. C 31 (8) (2011) 1809–1818.
[119] E. Długoń, K. Pach, M. Gawęda, R. Jadach, A. Wajda, M. Leśniak, A. Benko, M. Dziadek, M. Sowa, W. Simka, M. Sitarz, Anticorrosive ZrO2 and ZrO2-SiO2 layers on titanium substrates for biomedical applications, Surf. Coating. Technol. 331 (2017) 221–229.
[120] M.F. Tano de la Hoz, M.R. Katunar, A. González, A. Gomez Sanchez, A.O. Díaz, S. Ceré, Effect of anodized zirconium implants on early osseointegration process in adult rats: a histological and histomorphometric study, Prog. Biomater. 8 (4) (2019) 249–260.
[121] M.R. Katunar, A. Gomez Sanchez, A. Santos Coquillat, A. Civantos, E. Martinez Campos, J. Ballarre, T. Vico, M. Baca, V. Ramos, S. Cere, In vitro and in vivo characterization of anodised zirconium as a potential material for biomedical applications, Mater. Sci. Eng. C 75 (2017) 957–968.
[122] S.B. Farina, A.G. Sanchez, S. Ceré, Effect of surface modification on the corrosion resistance of Zr-2.5Nb as material for permanent implants, Procedia Materials Science 8 (2015) 1166–1173.
[123] S. Minagar, Y. Li, C.C. Berndt, C. Wen, The influence of titania–zirconia–zirconium titanate nanotube characteristics on osteoblast cell adhesion, Acta Biomater. 12 (2015) 281–289.
[124] D. Ionita, M. Vardaki, M.S. Stan, A. Dinischiotu, I. Demetrescu, Enhance stability and in vitro cell response to a bioinspired coating on Zr alloy with increasing chitosan content, J. Bionic Eng. 14 (3) (2017) 459–467.
[125] M.R. Kaluđerović, J.P. Schreckenbach, H.-L. Graf, Zirconia coated titanium for implants and their interactions with osteoblast cells, Mater. Sci. Eng. C 44 (2014) 254–261.
[126] S.L. Aktuğ, S. Durdu, E. Yalçın, K. Çavuşoğlu, M. Usta, In vitro properties of bioceramic coatings produced on zirconium by plasma electrolytic oxidation, Surf. Coating. Technol. 324 (2017) 129–139.
[127] F. Tana, E. De Giglio, S. Cometa, A. D'Agostino, A. Serafini, F. Variola, N. Bono, R. Chiesa, L. De Nardo, Ca-doped zirconia mesoporous coatings for biomedical applications: a physicochemical and biological investigation, J. Eur. Ceram. Soc. 40 (11) (2020) 3698–3706.
[128] L. Zhang, S. Zhu, Y. Han, C. Xiao, W. Tang, Formation and bioactivity of HA nanorods on micro-arc oxidized zirconium, Mater. Sci. Eng. C 43 (2014) 86–91.
[129] R. Quan, D. Yang, J. Yan, W. Li, X. Wu, H. Wang, Preparation of graded zirconia–CaP composite and studies of its effects on rat osteoblast cells in vitro, Mater. Sci. Eng. C 29 (1) (2009) 253–260.
[130] L.V. Tapia-Lopez, H.E. Esparza-Ponce, A. Luna-Velasco, P.E. Garcia-Casillas, H. Castro-Carmona, J.S. Castro, Bioactivation of zirconia surface with laminin protein coating via plasma etching and chemical modification, Surf. Coating. Technol. 402 (2020) 126307.
[131] S.L. Aktuğ, S. Durdu, E. Yalçın, K. Çavuşoğlu, M. Usta, Bioactivity and biocompatibility of hydroxyapatite-based bioceramic coatings on zirconium by plasma electrolytic oxidation, Mater. Sci. Eng. C 71 (2017) 1020–1027.
[132] X. Chen, Y. Li, P.D. Hodgson, C. Wen, In vitro behavior of human osteoblast-like cells (SaOS2) cultured on surface modified titanium and titanium–zirconium alloy, Mater. Sci. Eng. C 31 (7) (2011) 1545–1552.
[133] C.E. Wen, W. Xu, W.Y. Hu, P.D. Hodgson, Hydroxyapatite/titania sol–gel coatings on titanium–zirconium alloy for biomedical applications, Acta Biomater. 3 (3) (2007) 403–410.
[134] J. Michalska, M. Sowa, M. Piotrowska, M. Widziołek, G. Tylko, G. Dercz, R. P. Socha, A.M. Osyczka, W. Simka, Incorporation of Ca ions into anodic oxide coatings on the Ti-13Nb-13Zr alloy by plasma electrolytic oxidation, Mater. Sci. Eng. C 104 (2019) 109957.
[135] S. M, R. N, V. K, R.K. L, Fabrication, characterization and in-vitro evaluation of nanostructured zirconia/hydroxyapatite composite film on zirconium, Surf. Coating. Technol. 238 (2014) 58–67.
[136] A. Kazek-Kęsik, K. Pietryga, M. Basiaga, A. Blacha-Grzechnik, G. Dercz, I. Kalemba-Rec, E. Pamuła, W. Simka, Lactoferrin and collagen type I as components of composite formed on titanium alloys for bone replacement, Surf. Coating. Technol. 328 (2017) 1–12.
[137] W. Jing, M. Zhang, L. Jin, J. Zhao, Q. Gao, M. Ren, Q. Fan, Assessment of osteoinduction using a porous hydroxyapatite coating prepared by micro-arc oxidation on a new titanium alloy, Int. J. Surg. 24 (2015) 51–56.
[138] Y.-H. Jeong, H.-C. Choe, S.-W. Eun, Hydroxyapatite coating on the Ti–35Nb–xZr alloy by electron beam-physical vapor deposition, Thin Solid Films 519 (20) (2011) 7050–7056.
[139] H. Wang, T. Sun, L. Chang, F. Liu, B. Liu, C. Zhao, X. Xue, X. Xiong, Preparation of Ca doping ZrO2 coating on NiTi shape memory alloy by cathodic plasma electrolytic deposition and its structure, in-vitro bioactivity and biocompatibility analysis, Surf. Coating. Technol. 325 (2017) 136–144.
[140] B. Istrate, J.V. Rau, C. Munteanu, I.V. Antoniac, V. Saceleanu, Properties and in vitro assessment of ZrO2-based coatings obtained by atmospheric plasma jet spraying on biodegradable Mg-Ca and Mg-Ca-Zr alloys, Ceram. Int. 46 (10) (2020) 15897–15906.
[141] G. Wang, X. Liu, C. Ding, Phase composition and in-vitro bioactivity of plasma sprayed calcia stabilized zirconia coatings, Surf. Coating. Technol. 202 (24) (2008) 5824–5831.
[142] D. Faria, J.M. Pires, A.R. Boccaccini, O. Carvalho, F.S. Silva, J. Mesquita-Guimaraes, Development of novel zirconia implant's materials gradated design with improved bioactive surface, J. Mech. Behav. Biomed. Mater. 94 (2019) 110–125.
[143] B. Jiang, X. Hu, Z. Huang, Porous bio-ceramic coating on zirconia formed through freeze-drying, Mater. Lett. 109 (2013) 66–69.
[144] I.C. Lavos-Valereto, B. König, C. Rossa, E. Marcantonio, A.C. Zavaglia, A study of histological responses from Ti-6Al-7Nb alloy dental implants with and without plasma-sprayed hydroxyapatite coating in dogs, J. Mater. Sci. Mater. Med. 12 (3) (2001) 273–276.
[145] K. Pardun, L. Treccani, E. Volkmann, P. Streckbein, C. Heiss, G.L. Destri, G. Marletta, K. Rezwan, Mixed zirconia calcium phosphate coatings for dental

implants: tailoring coating stability and bioactivity potential, Mater. Sci. Eng. C 48 (2015) 337–346.
[146] A.I. Rubinstein, R.F. Sabirianov, F. Namavar, Enhanced cell growth by nanoengineering zirconia to stimulate electrostatic fibronectin activation, Nanotechnology 25 (6) (2014), 065101.
[147] Y. Cho, J. Hong, H. Ryoo, D. Kim, J. Park, J. Han, Osteogenic responses to zirconia with hydroxyapatite coating by aerosol deposition, J. Dent. Res. 94 (3) (2015) 491–499.
[148] H. Lee, S.M. Dellatore, W.M. Miller, P.B. Messersmith, Mussel-Inspired surface chemistry for multifunctional coatings, Science 318 (5849) (2007) 426–430.
[149] A. Oyane, M. Kakehata, I. Sakamaki, A. Pyatenko, H. Yashiro, A. Ito, K. Torizuka, Biomimetic apatite coating on yttria-stabilized tetragonal zirconia utilizing femtosecond laser surface processing, Surf. Coating. Technol. 296 (2016) 88–95.
[150] F.H. Schünemann, M.E. Galárraga-Vinueza, R. Magini, M. Fredel, F. Silva, J.C. M. Souza, Y. Zhang, B. Henriques, Zirconia surface modifications for implant dentistry, Mater. Sci. Eng. C 98 (2019) 1294–1305.
[151] M. Stefanic, K. Krnel, T. Kosmac, Novel method for the synthesis of a β-tricalcium phosphate coating on a zirconia implant, J. Eur. Ceram. Soc. 33 (15) (2013) 3455–3465.
[152] K. Schickle, J. Spitz, S. Neuss, R. Telle, Biomimetic in situ nucleation of calcium phosphates by protein immobilization on high strength ceramic materials, J. Eur. Ceram. Soc. 38 (1) (2018) 271–277.
[153] L. Bao, J. Liu, F. Shi, Y. Jiang, G. Liu, Preparation and characterization of TiO2 and Si-doped octacalcium phosphate composite coatings on zirconia ceramics (Y-TZP) for dental implant applications, Appl. Surf. Sci. 290 (2014) 48–52.
[154] M. Stefanic, K. Krnel, I. Pribosic, T. Kosmac, Rapid biomimetic deposition of octacalcium phosphate coatings on zirconia ceramics (Y-TZP) for dental implant applications, Appl. Surf. Sci. 258 (10) (2012) 4649–4656.
[155] X. Miao, Y. Hu, J. Liu, X. Huang, Hydroxyapatite coating on porous zirconia, Mater. Sci. Eng. C 27 (2) (2007) 257–261.
[156] K. Sakthiabirami, V.T. Vu, J.W. Kim, J.H. Kang, K.J. Jang, G.J. Oh, J.G. Fisher, K. D. Yun, H.P. Lim, S.W. Park, Tailoring interfacial interaction through glass fusion in glass/zinc-hydroxyapatite composite coatings on glass-infiltrated zirconia, Ceram. Int. 44 (14) (2018) 16181–16190.
[157] M.N. Aboushelib, R. Shawky, Osteogenesis ability of CAD/CAM porous zirconia scaffolds enriched with nano-hydroxyapatite particles, Int. J. Implant Dent. 3 (1) (2017) 21.
[158] S. Bose, D. Ke, A.A. Vu, A. Bandyopadhyay, S.B. Goodman, Thermal oxide layer enhances crystallinity and mechanical properties for plasma-sprayed hydroxyapatite biomedical coatings, ACS Appl. Mater. Interfaces 12 (30) (2020) 33465–33472.
[159] M. Berni, G. Marchiori, A. Gambardella, M. Boi, M. Bianchi, A. Russo, A. Visani, M. Marcacci, P.G. Pavan, N.F. Lopomo, Effects of working gas pressure on zirconium dioxide thin film prepared by pulsed plasma deposition: roughness, wettability, friction and wear characteristics, J. Mech. Behav. Biomed. Mater. 72 (2017) 200–208.
[160] A. Pelaez-Vargas, D. Gallego-Perez, M. Magallanes-Perdomo, M.H. Fernandes, D. J. Hansford, A.H. De Aza, P. Pena, F.J. Monteiro, Isotropic micropatterned silica coatings on zirconia induce guided cell growth for dental implants, Dent. Mater. 27 (6) (2011) 581–589.
[161] A. Jemat, M.J. Ghazali, M. Razali, Y. Otsuka, A. Rajabi, Effects of TiO2 on microstructural, mechanical properties and in-vitro bioactivity of plasma sprayed yttria stabilised zirconia coatings for dental application, Ceram. Int. 44 (4) (2018) 4271–4281.
[162] A. Balamurugan, G. Balossier, S. Kannan, J. Michel, J. Faure, S. Rajeswari, Electrochemical and structural characterisation of zirconia reinforced hydroxyapatite bioceramic sol–gel coatings on surgical grade 316L SS for biomedical applications, Ceram. Int. 33 (4) (2007) 605–614.
[163] E. Marin, M. Zanocco, F. Boschetto, M. Santini, W. Zhu, T. Adachi, E. Ohgitani, B. J. McEntire, B.S. Bal, G. Pezzotti, Silicon nitride laser cladding: a feasible technique to improve the biological response of zirconia, Mater. Des. 191 (2020) 108649.
[164] N.M. Zain, R. Hussain, M.R. Abdul Kadir, Quinone-rich polydopamine functionalization of yttria stabilized zirconia for apatite biomineralization: the effects of coating temperature, Appl. Surf. Sci. 346 (2015) 317–328.
[165] N.M. Zain, R. Hussain, M.R.A. Kadir, Surface modification of yttria stabilized zirconia via polydopamine inspired coating for hydroxyapatite biomineralization, Appl. Surf. Sci. 322 (2014) 169–176.
[166] Y.-T. Liu, T.-M. Lee, T.-S. Lui, Enhanced osteoblastic cell response on zirconia by bio-inspired surface modification, Colloids Surf. B Biointerfaces 106 (2013) 37–45.
[167] M. Liu, J. Zhou, Y. Yang, M. Zheng, J. Yang, J. Tan, Surface modification of zirconia with polydopamine to enhance fibroblast response and decrease bacterial activity in vitro: a potential technique for soft tissue engineering applications, Colloids Surf. B Biointerfaces 136 (2015) 74–83.
[168] G. Soon, B. Pingguan-Murphy, K.W. Lai, S.A. Akbar, Review of zirconia-based bioceramic: surface modification and cellular response, Ceram. Int. 42 (11) (2016) 12543–12555.
[169] E. Fernandez-Garcia, X. Chen, C.F. Gutierrez-Gonzalez, A. Fernandez, S. Lopez-Esteban, C. Aparicio, Peptide-functionalized zirconia and new zirconia/titanium biocermets for dental applications, J. Dent. 43 (9) (2015) 1162–1174.
[170] S.-K. Hsu, P.-L. Chang, W.-F. Ho, H.-C. Hsu, H.-J. Liao, S.-C. Wu, Osteogenesis ability of biomimetic modified 3Y-TZP ceramic using chemical treatment, Thin Solid Films 596 (2015) 118–127.
[171] H. Aita, N. Hori, M. Takeuchi, T. Suzuki, M. Yamada, M. Anpo, T. Ogawa, The effect of ultraviolet functionalization of titanium on integration with bone, Biomaterials 30 (6) (2009) 1015–1025.
[172] T. Tuna, M. Wein, B. Altmann, T. Steinberg, J. Fischer, W. Att, Effect of ultraviolet photofunctionalisation on the cell attractiveness of zirconia implant materials, Eur. Cell. Mater. 29 (2015) 82–94. ; discussion 95-6.
[173] M. Brezavšček, A. Fawzy, M. Bächle, T. Tuna, J. Fischer, W. Att, The effect of UV treatment on the osteoconductive capacity of zirconia-based materials, Materials 9 (12) (2016) 958.
[174] A. Mehjabeen, T. Song, W. Xu, H.P. Tang, M. Qian, Zirconium Alloys for Orthopaedic and Dental Applications, Adv. Eng. Mater. 20 (9) (2018) 1800207.
[175] L. Nie, Y. Zhan, H. Liu, C. Tang, Novel β-type Zr–Mo–Ti alloys for biological hard tissue replacements, Mater. Des. 53 (2014) 8–12.
[176] T. Guo, K. Gulati, Z. Shen, P. Han, Z. Fan, Therapeutic outcomes of non-grafted and platelet concentrations-grafted transcrestal maxillary sinus elevation (TSFE): a systematic review and meta-analysis, Sci. Rep. 10 (2020) 1–12.
[177] H.M. Grandin, S. Berner, M. Dard, A review of titanium zirconium (TiZr) alloys for use in endosseous dental implants, Materials 5 (8) (2012) 1348–1360.
[178] X.-B. Chen, A. Nouri, P. Hodgson, C. Wen, Surface modification of TiZr alloy for biomedical application, Adv. Mater. Res. 15–17 (2007) 89–94.
[179] S. Grigorescu, C. Ungureanu, R. Kirchgeorg, P. Schmuki, I. Demetrescu, Various sized nanotubes on TiZr for antibacterial surfaces, Appl. Surf. Sci. 270 (2013) 190–196.
[180] J. Hu, J. Lin, Y. Zhang, Z. Lin, Z. Qiao, Z. Liu, W. Yang, X. Liu, M. Dong, Z. Guo, A new anti-biofilm strategy of enabling arbitrary surfaces of materials and devices with robust bacterial anti-adhesion via a spraying modified microsphere method, J. Mater. Chem. 7 (45) (2019) 26039–26052.
[181] D. Martinez-Marquez, K. Gulati, C.P. Carty, R.A. Stewart, S. Ivanovski, Determining the relative importance of titania nanotubes characteristics on bone implant surface performance: a quality by design study with a fuzzy approach, Mater. Sci. Eng. C 114 (2020) 110995.
[182] K. Gulati, S. Maher, D.M. Findlay, D. Losic, Titania nanotubes for orchestrating osteogenesis at the bone-implant interface, Nanomedicine 11 (14) (2016) 1847–1864.
[183] P.D. Charles, P.A. Anandapandian, S. Samuel, Osteogenic potential of laser modified and conditioned titanium zirconium surfaces, J. Indian Prosthodont. Soc. 16 (3) (2016) 253–258.
[184] I.d.S.V. Marques, V.A.R. Barão, N.C.d. Cruz, J.C.-C. Yuan, M.F. Mesquita, A. P. Ricomini-Filho, C. Sukotjo, M.T. Mathew, Electrochemical behavior of bioactive coatings on cp-Ti surface for dental application, Corrosion Sci. 100 (2015) 133–146.
[185] J. Cordeiro, H. Pantaroto, E. Paschoaleto, E. Rangel, N. Cruz, C. Sukotjo, V. Barao, Synthesis of biofunctional coating for a TiZr alloy: surface, electrochemical, and biological characterizations, Appl. Surf. Sci. 452 (2018) 268–278.
[186] J. Kim, Y.C. Choi, H.S. Kim, S.I. Hong, Biomimetic deposition of apatite on Zr-1Nb and Ti-6Al-4V, Mater. Sci. Forum 534–536 (2007) 1013–1016.
[187] L. Jonásová, F.A. Müller, A. Helebrant, J. Strnad, P. Greil, Biomimetic apatite formation on chemically treated titanium, Biomaterials 25 (7–8) (2004) 1187–1194.
[188] C. Gross, T. Bergfeldt, T. Fretwurst, R. Rothweiler, K. Nelson, A. Stricker, Elemental analysis of commercial zirconia dental implants - is “metal-free” devoid of metals? J. Mech. Behav. Biomed. Mater. 107 (2020) 103759.
[189] H. Nishihara, M. Haro Adanez, W. Att, Current status of zirconia implants in dentistry: preclinical tests, J. Prosthodont. Res. 63 (1) (2019) 1–14.
[190] K. Kniha, H. Kniha, S.C. Möhlhenrich, S. Milz, F. Hölzle, A. Modabber, Papilla and alveolar crest levels in immediate versus delayed single-tooth zirconia implants, Int. J. Oral Maxillofac. Surg. 46 (8) (2017) 1039–1044.
[191] S. Ramesh, K.Y. Sara Lee, C.Y. Tan, A review on the hydrothermal ageing behaviour of Y-TZP ceramics, Ceram. Int. 44 (17) (2018) 20620–20634.
[192] P.F. Manicone, P. Rossi Iommetti, L. Raffaelli, An overview of zirconia ceramics: basic properties and clinical applications, J. Dent. 35 (11) (2007) 819–826.
[193] R.-J. Kohal, W. Att, M. Bächle, F. Butz, Ceramic abutments and ceramic oral implants. An update, Periodontol. 2000 47 (1) (2008) 224–243.
[194] M. Hisbergues, S. Vendeville, P. Vendeville, Zirconia: established facts and perspectives for a biomaterial in dental implantology, J. Biomed. Mater. Res. B 88B (2) (2009) 519–529.
[195] S. Pieralli, R.J. Kohal, R.E. Jung, K. Vach, B.C. Spies, Clinical outcomes of zirconia dental implants: a systematic review, J. Dent. Res. 96 (1) (2017) 38–46.
[196] S. Roehling, K.A. Schlegel, H. Woelfler, M. Gahlert, Performance and outcome of zirconia dental implants in clinical studies: a meta-analysis, Clin. Oral Implants Res. 29 (S16) (2018) 135–153.
[197] M. Rahmati, M. Mozafari, A critical review on the cellular and molecular interactions at the interface of zirconia-based biomaterials, Ceram. Int. 44 (14) (2018) 16137–16149.
[198] A. Naveau, C. Rignon-Bret, C. Wulfman, Zirconia abutments in the anterior region: a systematic review of mechanical and esthetic outcomes, J. Prosthet. Dent 121 (5) (2019) 775–781, e1.
[199] A. Biesiekierski, J. Wang, M. Abdel-Hady Gepreel, C. Wen, A new look at biomedical Ti-based shape memory alloys, Acta Biomater. 8 (5) (2012) 1661–1669.
[200] B. Möller, H. Terheyden, Y. Açil, N.M. Purcz, K. Hertrampf, A. Tabakov, E. Behrens, J. Wiltfang, A comparison of biocompatibility and osseointegration of ceramic and titanium implants: an in vivo and in vitro study, Int. J. Oral Maxillofac. Surg. 41 (5) (2012) 638–645.

[201] A. Lennartz, A. Dohmen, S. Bishti, H. Fischer, S. Wolfart, Retrievability of implant-supported zirconia restorations cemented on zirconia abutments, J. Prosthet. Dent 120 (5) (2018) 740–746.
[202] R.J. Kohal, S.B. Patzelt, F. Butz, H. Sahlin, One-piece zirconia oral implants: one-year results from a prospective case series. 2. Three-unit fixed dental prosthesis (FDP) reconstruction, J. Clin. Periodontol. 40 (5) (2013) 553–562.
[203] O. Hoffmann, N. Angelov, G.G. Zafiropoulos, S. Andreana, Osseointegration of zirconia implants with different surface characteristics: an evaluation in rabbits, Int. J. Oral Maxillofac. Implants 27 (2) (2012) 352–358.
[204] J. Becker, G. John, K. Becker, S. Mainusch, G. Diedrichs, F. Schwarz, Clinical performance of two-piece zirconia implants in the posterior mandible and maxilla: a prospective cohort study over 2 years, Clin. Oral Implants Res. 28 (1) (2017) 29–35.
[205] C. Piconi, G. Maccauro, Zirconia as a ceramic biomaterial, Biomaterials 20 (1) (1999) 1–25.
[206] D. Mints, C. Elias, P. Funkenbusch, L. Meirelles, Integrity of implant surface modifications after insertion, Int. J. Oral Maxillofac. Implants 29 (1) (2014) 97–104.
[207] M. Tsumita, Y. Kokubo, T. Kano, K. Sasaki, The effect of fatigue loading on the screw joint stability of zirconium abutment, J. Prosthodont. Res. 57 (3) (2013) 219–223.
[208] P. Corne, P. De March, F. Cleymand, J. Geringer, Fretting-corrosion behavior on dental implant connection in human saliva, J. Mech. Behav. Biomed. Mater. 94 (2019) 86–92.
[209] N. Barati, A. Yerokhin, F. Golestanifard, S. Rastegari, E.I. Meletis, Alumina-zirconia coatings produced by Plasma Electrolytic Oxidation on Al alloy for corrosion resistance improvement, J. Alloys Compd. 724 (2017) 435–442.
[210] L. Semetse, B.A. Obadele, L. Raganya, J. Geringer, P.A. Olubambi, Fretting corrosion behaviour of Ti-6Al-4V reinforced with zirconia in foetal bovine serum, J. Mech. Behav. Biomed. Mater. 100 (2019) 103392.
[211] S.E. Elsaka, A.M. Elnaghy, Mechanical properties of zirconia reinforced lithium silicate glass-ceramic, Dent. Mater. 32 (7) (2016) 908–914.
[212] Y. Hemberger, C. Berthold, K.G. Nickel, Wetting and corrosion of yttria stabilized zirconia by molten slags, J. Eur. Ceram. Soc. 32 (11) (2012) 2859–2866.
[213] J. Chevalier, What future for zirconia as a biomaterial? Biomaterials 27 (4) (2006) 535–543.
[214] H. Tong, C.B. Tanaka, M.R. Kaizer, Y. Zhang, Characterization of three commercial Y-TZP ceramics produced for their high-translucency, high-strength and high-surface area, Ceram. Int. 42 (1 Pt B) (2016) 1077–1085.
[215] F. Zhang, B.C. Spies, J. Vleugels, H. Reveron, C. Wesemann, W.-D. Müller, B. van Meerbeek, J. Chevalier, High-translucent yttria-stabilized zirconia ceramics are wear-resistant and antagonist-friendly, Dent. Mater. 35 (12) (2019) 1776–1790.
[216] B.C. Spies, A. Fross, E. Adolfsson, A. Bagegni, S. Doerken, R.J. Kohal, Stability and aging resistance of a zirconia oral implant using a carbon fiber-reinforced screw for implant-abutment connection, Dent. Mater. 34 (10) (2018) 1585–1595.
[217] M. Ye, B. Shi, Zirconia nanoparticles-induced toxic effects in osteoblast-like 3T3-E1 cells, Nanoscale Res Lett 13 (1) (2018) 353, 353.
[218] X. He, F.-X. Reichl, Y. Wang, B. Michalke, S. Milz, Y. Yang, P. Stolper, G. Lindemaier, M. Graw, R. Hickel, C. Högg, Analysis of titanium and other metals in human jawbones with dental implants – a case series study, Dent. Mater. 32 (8) (2016) 1042–1051.